当科における非機能性膵神経内分泌腫瘍切除症例15例の検討	示説	石黒保直、佐久間康成、笹沼英紀、佐田尚宏、安田是和, 齋藤倫寛、福嶋敬宜	第26回日本肝胆膵外科学会・学術集会	2014年6月12日 和歌山県	国内
EUS-FNAで診断した非機能性微細PNETの2例	口頭	牛尾純, 横山健介, 沼尾規且, 畑中恒, 冨山剛, 玉田喜一, 福嶋敬宜, 佐田尚宏, 山	第24回東京膵臓研究会	2014年5月24日 東京	国内
膵神経内分泌腫瘍(NET)の病理診断	口頭発表・シンポジウムS1-2	大池信之	第18回日本内分泌病理学会学術総会	2014年11月1-2日 東京都千代田区	国内
膵神経内分泌腫瘍の診断とその問題点	口頭発表・ランチョンセミナー	大池信之	第60回日本病理学会秋期特別総会	2014年11月20-21日 沖縄県浦添市	国内
膵mixed ductal-neuroendocrine carcinomaの3切除例	口頭発表・一般演題17	大池信之、初鹿野誠也、司馬真一、磯辺友秀、広田由子、塩川章	第19回日本外科病理学会学術集会	2014年11月14-15日 沖縄県南風原町	国内
胃癌におけるmTOR発現の特徴	ポスター上部消化管6	田中雄也, 岩渕三哉, 小菅優子	第103回日本病理学会総会	2014年4月24-26日 広島市	国内
消化管内分泌細胞腫瘍の病理	特別講演	岩渕三哉	栃木県立がんセンター グランドカンファランス	2014年6月19日 宇都宮市	国内
膵神経内分泌腫瘍の一例	口頭	西田浩彰, 本間慶一, 川崎 隆, 岩渕三哉, 須藤真則, 船越和博	第79回日本病理学会東北支部総会/学術集会	2014年7月19-20日 盛岡市	国内
消化管内分泌細胞腫瘍の病理－特性、分類、診断－	特別講演	岩渕三哉	Gastroenterology Seminor in Kurume	2014年9月3日 久留米市	国内
神経内分泌腫瘍の病理診断:現状と課題 消化管神経内分泌腫瘍の病理診断:現状と課題	シンポジウム1	岩渕三哉, 田中雄也, 小菅優子, 渡辺 徹	第18回日本内分泌病理学会学術総会	2014年11月1-2日 東京都千代田区	国内
全エクソームシーケンス解析からわかってきた胃癌の遺伝子変異と臨床病理	ワークショップWS-6-4	牛久哲男、石川俊平、垣内美和子、阿部浩幸、油谷浩幸、深山正久	第103回日本病理学会総会	2014年4月25日 広島市	国内
ワークショップ9(本邦におけるNET 治療の実態—診療ガイドラインへの展開—) 本邦におけるNET治療の実際－診療ガイドラインへの展望—	口頭	伊藤鉄英	第114回日本外科学会定期学術集会	2014年4月3-5日 京都市	国内
シンポジウム2(内分泌腫瘍に対する治療) 膵NETの現状と内科的治療	口頭	伊藤鉄英	第26回日本内分泌外科学会総会	2014年5月22-23日 名古屋市	国内
International Session 2 ／ インターナショナルセッション 2 Epidemiological status of pancreatic and gastrointestinal neuroendocrine tumors in Japan 我が国における膵消化管神経内分泌腫瘍の現況	口頭	伊藤鉄英	第12回日本臨床腫瘍学会学術集会	2014年7月17-19日 福岡市	国内
ワークショップ16(消化器における神経内分泌腫瘍) 神経内分泌腫瘍(NEC)の本邦疫学調査結果と治療展望	口頭	五十嵐久人、肱岡真之、伊藤鉄英	第22回 JDDW(第56回消化器病学会大会)	2014年10月23-26日 神戸市	国内
Clinical Aspects of pNET	口頭	Ito T.	45th Anniversary Meeting American Pancreatic Association	2014.11.5-8 Hawaii	国外

Aktの新規抑制因子をコードするPHLDA3遺伝子は神経内分泌腫瘍のがん抑制遺伝子である	ポスター 基礎研究P1-1	大木理恵子	第2回日本神経内分泌腫瘍研究会学術集会	2014年9月20日 東京都文京区	国内
PH domain-only protein PHLDA3 is a novel p53-regulated repressor of Akt and a novel tumor suppressor of neuroendocrine tumors	シンポジウム発表 SS-6	大木理恵子	日本癌学会年会	2014年9月27日 神奈川県横浜市	国内
PHLDA3は膵神経内分泌腫瘍の新規がん抑制遺伝子である	ポスター発表 P-3295	山口 陽子、陳 ヨ、西川 雷羅、峯岸 舞子、大木理恵子	日本癌学会年会	2014年9月27日 神奈川県横浜市	国内
Aktの新規抑制因子をコードするPHLDA3遺伝子は神経内分泌腫瘍のがん抑制遺伝子である	口頭発表	大木理恵子	アステラス病態代謝研究会	2014年10月18日 東京都中央区	国内
PH domain-only protein PHLDA3 is a novel p53-regulated repressor of Akt and a novel tumor suppressor of neuroendocrine tumors	口頭発表	大木理恵子	日独がんワークショップ	2014年11月15日 ドイツベルリン	国外
PH domain-only protein PHLDA3 is a novel p53-regulated repressor of Akt and a novel tumor suppressor of neuroendocrine tumors	口頭発表	大木理恵子	日韓がんワークショップ	2014年11月29日 韓国済州島	国外
十二指腸内分泌腫瘍に対する至適術式の検討 特に膵頭十二指腸切除の要否について	ポスター発表 P87-4	岩崎 寿光, 奈良 聡, 巌 康仁, 須藤 広誠, 岸 庸二, 江崎 稔, 島田 和明, 小菅 智男	第26回日本肝胆膵外科学会学術集会	2014年6月11-13日 和歌山市	国内

2. 学会誌・雑誌等における論文掲載

掲載した論文(発表題目)	発表者氏名	発表した場所(学会誌・雑誌等名)	発表した時期	国内・外の別
Streptozocin chemotherapy for advanced/metastatic well-differentiated neuroendocrine tumors: an analysis of a multi-center survey in Japan.	Aoki T, Kokudo N, Komoto I, Takaori K, Kimura W, Sano K, Takamoto T, Hashimoto T, Okusaka T, Morizane C, Ito T, Imamura M.	J Gastroenterol.	[Epub ahead of print]	国外
Multicenter retrospective analysis of systemic chemotherapy for advanced neuroendocrine carcinoma of the digestive system.	Yamaguchi T, Machida N, Morizane C, Kasuga A, Takahashi H, Sudo K, Nishina T, Tobimatsu K, Ishido K, Furuse J, Boku N, Okusaka T.	Cancer Sci,	2014 Jun, 105:1176-1181.	国外
Does the WHO 2010 classification of pancreatic neuroendocrine neoplasms accurately characterize pancreatic neuroendocrine carcinomas?	Hijioka, S.Hosoda, W.Mizuno, N. Hara, K.Imaoka, H.Bhatia, V.Mekky, M. A.Tajika, M.Tanaka, T.Ishihara, M.Yogi, T.Tsutumi, H.Fujiyoshi, T. Sato, T.Hieda, N.Yoshida, T.Okuno, N.Shimizu, Y.Yatabe, Y.Niwa, Y.Yamao, K.	J Gastroenterol	2014 Aug 21. [Epub ahead of print]	国外
A case of mixed adenoneuroendocrine carcinoma of the gallbladder arising from an intracystic papillary neoplasm associated with pancreaticobiliary maljunction.	Meguro Y, Fukushima N, Koizumi M, Kasahara N, Hydo M, Morishima K, Sata N, Lefor AT, Yasuda Y.	Pathol Int.	2014 Sep; 64(9):465-71	国外
第1章2. 神経内分泌腫瘍のWHO分類2010	福嶋敬宜	これだけは知っておきたい膵疾患診療の手引き(花田敬士編), 中外医学社, 東京	2014, pp14-20	国内
Calculation of the Ki67 index in pancreatic neuroendocrine tumors: a comparative analysis of four counting methodologies.	Reid MD, Bagci P, Ohike N, Saka B, Erbarut Seven I, Dursun N, Balci S, Gucer H, Jang KT, Tajiri T, Basturk O, Kong SY, Goodman M, Akkas G, Adsay V.	Mod Pathol.	2014 Nov 21. doi: 10.1038/modpathol.2014.156. [Epub ahead of print]	国外
胃内分泌細胞癌	岩渕三哉, 渡辺徹, 須貝美佳	臨床医のための胃がん病理アトラス. 安井弥, 北島政樹, 吉田和弘(監), 東京, メディカルビュー社,	2014:135-143 (2014.9.10)	国内
同一病巣内に神経内分泌腫瘍と腺癌の成分を認めた径8mmの直腸腫瘍の1例	木戸知紀, 島田能史, 中野麻恵, 中野雅人, 亀山仁史, 野上仁, 若井俊文, 岩渕三哉	日本大腸肛門病学会雑誌	2015; Jan, 68(1):55-59.	国内
大腸の神経内分泌腫瘍の病理診断	岩渕三哉, 須貝美佳	大腸疾患NOW 2015. 杉原健一, 五十嵐正広, 渡邉聡明, 大倉康男(編), 東京, 日本メディカルセン	2015:61-75, (2015.1.20)	国内
Epidemiological trends of pancreatic and gastrointestinal neuroendocrine tumors in Japan: a nationwide survey analysis.	Ito T, Igarashi H, Nakamura K, Sasano H, Okusaka T, Yakano K, Komoto I, Tanaka M, Imamura M, Jensen RT, Takayanagi R, Shimatsu A.	J Gastroenterol.	2015 Jan,50:58-64.	国外
Example of the important of case reports/case series in advancement of medicine in rare diseases: using their role in neuroendocrine tumors as an example.	Nakamura T, Igarashi H, Ito T, Jensen RT.	World J Clin Cases.	2014 Nov,2:608-13.	国外
A synchronous pancreatic neuroendocrine tumor and duodenal gastrointestinal stromal tumor.	Ueda K, Hisato I, Niina Y, Hijioka M, Lee L, Osoegawa T, Nakamura K, Shinichi A, Ohtsuka T, Tanaka M, Takayanagi R, Ito T.	Intern Med.	2014 Nov,53:2483-8.	国外

Serum chromogranin A is a useful marker for Japanese patients with pancreatic neuroendocrine tumors.	Hijioka M, Ito T, Igarashi H, Fujimori N, Lee L, Nakamura T, Jensen RT, Takayanagi R.	Cancer Sci.	2014 Nov,105:1464-71.	国外
Necrolytic migratory erythema associated with alteration from predominantly gastrin-secreting to predominantly glucagon-secreting pancreatic neuroendocrine tumor.	Kido-Nakahara M, Nakahara T, Miki M, Igarashi H, Ito T, Furue M.	Eur J Dermatol.	2014 Oct 21,[Epub ahead of print]	国外
PHLDA3 is a novel tumor suppressor of neuroendocrine tumors	Ohki R, Saito K, Chen Y, Kawase T, Hiraoka N, Saigawa R, Minegishi M, Aita Y, Yanai G, Shimizu H, Yachida S, Sakata N, Doi R, Kosuge T, Shimada K, Tycko B, Tsukada T, Kanai Y, Sumi S, Namiki H, Taya Y, Shibata T, Nakagama H.	Proc Natl Acad Sci U S A	2014, May 111(23):E2404-13.	国外
新規がん抑制遺伝子PHLDA3によるAkt経路の制御機構と治療への展開 −膵神経内分泌腫瘍の個別化医療開発を目指して−	山口 陽子, 斉藤 梢, 陳 ヨ, 大木 理恵子	実験医学	2014; 7月増刊号: 135-143	国内
Basing treatment strategy for non-functional pancreatic neuroendocrine tumors on tumor size.	Kishi Y, Shimada K, Nara S, Esaki M, Hiraoka N, Kosuge T.	Ann Surg Oncol,	21(9):2882-8, 2014	国外

IV. 研究成果の刊行物・別刷

Cancer Science
Japanese Cancer Association JCA
Open Access

Multicenter retrospective analysis of systemic chemotherapy for advanced neuroendocrine carcinoma of the digestive system

Tomohiro Yamaguchi,[1,2] Nozomu Machida,[3] Chigusa Morizane,[1] Akiyoshi Kasuga,[4] Hideaki Takahashi,[5] Kentaro Sudo,[6] Tomohiro Nishina,[7] Kazutoshi Tobimatsu,[8] Kenji Ishido,[9] Junji Furuse,[10] Narikazu Boku[11] and Takuji Okusaka[1]

[1]Department of Hepatobiliary and Pancreatic Oncology, National Cancer Center Hospital, Tokyo; [2]Department of Biostatics and Epidemiology, Graduate School of Medicine, Yokohama City University, Kanagawa; [3]Division of Gastrointestinal Oncology, Shizuoka Cancer Center, Shizuoka; [4]Hepatobiliary and Pancreatic Division, Cancer Institute Hospital, Tokyo; [5]Department of Hepatobiliary and Pancreatic Oncology, National Cancer Center Hospital East, Chiba; [6]Division of Gastrointestinal Oncology, Chiba Cancer Center, Chiba; [7]Department of Gastrointestinal Medical Oncology, Shikoku Cancer Center, Ehime; [8]Department of Gastroenterological Oncology, Hyogo Cancer Center, Hyogo; [9]Department of Gastroenterology, Kitasato University School of Medicine, Kanagawa; [10]Department of Medical Oncology, Kyorin University School of Medicine, Tokyo; [11]Department of Clinical Oncology, St. Marianna University School of Medicine, Kanagawa, Japan

Key words

Cisplatin, digestive system, etoposide, irinotecan, neuroendocrine carcinoma

Correspondence

Chigusa Morizane, Department of Hepatobiliary and Pancreatic Oncology, National Cancer Center Hospital, 5-1-1 Tsukiji, Chuo-ku, Tokyo 104-0045, Japan.
Tel: +81-3-3542-2511; Fax: +81-3-3542-3815;
E-mail: cmorizan@ncc.go.jp

Funding information

National Cancer Center Research and Development Fund (23-A-22).

Received February 15, 2014; Revised June 11, 2014; Accepted June 24, 2014

Cancer Sci **105** (2014) 1176–1181

doi: 10.1111/cas.12473

This study analyzed outcomes of systemic chemotherapy for advanced neuroendocrine carcinoma (NEC) of the digestive system. Clinical data from 258 patients with unresectable or recurrent NEC of the gastrointestinal tract (GI) or hepato-biliary-pancreatic system (HBP), who received chemotherapy, were collected from 23 Japanese institutions and analyzed retrospectively. Patients had primary sites in the esophagus (n = 85), stomach (n = 70), small bowel (n = 6), colorectum (n = 31), hepato-biliary system (n = 31) and pancreas (n = 31). Median overall survival (OS) was 13.4 months the esophagus, 13.3 months for the stomach, 29.7 months for the small bowel, 7.6 months for the colorectum, 7.9 months for the hepato-biliary system and 8.5 months for the pancreas. Irinotecan plus cisplatin (IP) and etoposide plus cisplatin (EP) were most commonly selected for GI-NEC and HBP-NEC. For patients treated with IP/EP (n = 160/46), the response rate was 50/28% and median OS was 13.0/7.3 months. Multivariate analysis among patients treated with IP or EP showed that the primary site (GI *vs* HBP; hazard ratio [HR] 0.58, 95% confidence interval [CI] 0.35–0.97) and baseline serum lactate dehydrogenase levels (not elevated *vs* elevated; HR 0.65, 95% CI 0.46–0.94) were independent prognostic factors for OS, while the efficacy of IP was slightly better than for EP (HR 0.80, 95% CI 0.48–1.33; P = 0.389). IP and EP are the most common treatment regimens for NEC of the digestive system. HBP primary sites and elevated lactate dehydrogenase levels are unfavorable prognostic factors for survival. A randomized controlled trial is required to establish the appropriate chemotherapy regimen for advanced NEC of the digestive system. This study was registered at UMIN as trial number 000005176.

Neuroendocrine neoplasms (NEN) are rare tumors that exhibit a variety of morphological, functional and behavioral characteristics.[1] The World Health Organization (WHO) has proposed a grading system for NEN that divides them into three categories based on proliferation as follows: (i) neuroendocrine tumor (NET) (G1) with a mitotic count of <2/10 high power fields (HPF) and/or a Ki-67 index of ≤2%; (ii) NET (G2) with a mitotic count of 2–20/10 HPF and/or a Ki-67 index of 3–20%; and (iii) neuroendocrine carcinoma (NEC) with a mitotic count of >20/10 HPF and/or a Ki-67 index of >20%.[2] Among the three categories, NEC is a poorly differentiated, high-grade malignant tumor, previously termed poorly differentiated neuroendocrine carcinoma (PDNEC), including small-cell carcinoma (SCC) and large-cell NEC. The primary sites of NEC are varied in many organs, with NEC arising in the digestive system accounting for 20–68% of cases with extra-pulmonary NEC.[3–7]

In treating advanced extra-pulmonary NEC, guidelines recommend chemotherapy regimens, which are suitable for small-cell lung carcinoma (SCLC).[8–10] Therefore, platinum-containing regimens, such as etoposide plus cisplatin (EP), are commonly used for NEC arising from the digestive system in clinical practice worldwide and irinotecan plus cisplatin (IP) is commonly adopted in Japan. However, no randomized controlled trial has been conducted previously and retrospective reports have been limited in scope and number.[11–15] Therefore, we conducted a multicenter retrospective study on the outcomes of systemic chemotherapy for advanced NEC of the digestive system to obtain useful information to prepare for a future clinical trial.

Materials and Methods

The selection criteria were as follows: (i) a histologically proven NEC such as PDNEC, SCC, mixed endocrine-exocrine carcinoma with a PDNEC component (MEEC), or a neuroendocrine tumor with a rapidly progressive clinical course (clinically-diagnosed NEC); (ii) a primary tumor arising in the digestive system (gastrointestinal tract [GI] or hepato-biliary-pancreatic system [HBP]); (iii) an unresectable or recurrent disease treated with systemic chemotherapy, which was initiated between April 2000 and March 2011; and (iv) no prior treatment, except for surgical resection. Data were collected from the medical records of patients at 23 institutions in Japan using a standardized data collection form. This study was approved by the institutional review boards of the participating institutions and registered with the UMIN Clinical Trials Registry as UMIN 000005176 (http://www.umin.ac.jp/ctr/).

Responses were evaluated according to Response Evaluation Criteria in Solid Tumors (RECIST), version 1.1. Progression-free survival (PFS) was defined as the time from initiation of chemotherapy to confirmation of disease progression or death due to any cause. Overall survival (OS) was defined as the time from initiation of chemotherapy to death due to any cause. Surviving patients were censored on their last follow-up date. PFS and OS were estimated using the Kaplan–Meier method and compared with the log-rank test. Among the patients treated with EP or IP, multiple variate analysis by Cox proportional hazard models was performed, and the hazard ratio (HR) and the corresponding 95% confidence interval (95% CI) for OS were calculated, using the following seven variables selected based on the results of previous investigations and our clinical experience: age (<60 years/≥60 years), sex (male/female), Eastern Cooperative Oncology Group performance status (0–1/≥2), primary site (GI/HBP), liver metastasis (yes/no), prior surgery (yes/no), baseline serum lactate dehydrogenase (LDH) levels (not elevated/elevated), and first-line chemotherapy regimens (EP/IP). Statistical analysis was performed using SPSS software, version 17.0 (SPSS, Chicago, IL, USA).

Results

Patient characteristics. Figure 1 represents the study population flow chart. A total of 258 patients satisfied the selection criteria. Their characteristics are shown in Table 1. The majority of patients were male (71%) and the most common primary site was the esophagus (33%) followed by the stomach (27%). Most patients both in the GI (84%) and HBP (88%) subgroups had Stage IV or recurrent disease.

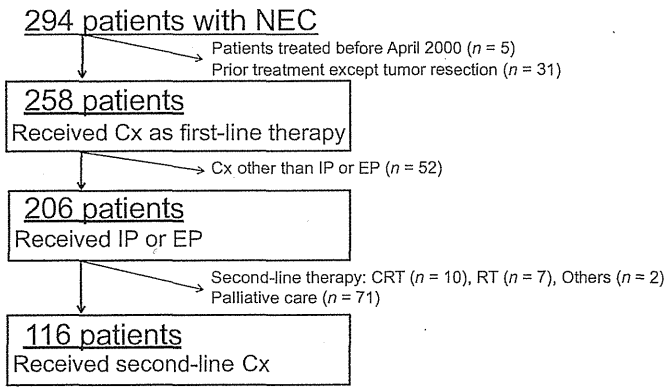

Fig. 1. Flow chart of the study population. CRT, chemoradiotherapy; Cx, chemotherapy; EP, etoposide plus cisplatin; IP, irinotecan plus cisplatin; *n*, number; NEC, neuroendocrine carcinoma; RT, radiotherapy.

Table 1. Patient characteristics

	All patients	GI primary	HBP primary
Number	258	192 (74%)	66 (26%)
Age, years			
Median (range)	62.5 (26–81)	63 (26–81)	58.5 (29–78)
Sex (%)			
Male	182 (71)	153 (80)	29 (44)
Female	76 (29)	39 (20)	37 (56)
Performance status (%)			
0 or 1	240 (93)	176 (92)	64 (97)
≧2	18 (7)	16 (8)	2 (3)
Baseline lactate dehydrogenase (%)			
Elevated	136 (53)	91 (47)	45 (68)
Not elevated	95 (37	79 (41)	16 (24)
No data	27 (10)	22 (11)	5 (8)
Chromogranin A staining (%)			
Positive	172 (67)	122 (64)	50 (76)
Negative	59 (23)	51 (26)	8 (12)
No data	27 (10)	19 (10)	8 (12)
Synaptophysin staining (%)			
Positive	204 (79)	153 (80)	51 (77)
Negative	29 (11)	21 (11)	8 (12)
No data	25 (10)	18 (9)	7 (11)
Ki-67 index (%)			
≧55%	43 (17)	20 (10)	23 (35)
>20%, <55%	27 (10)	18 (9)	9 (14)
No data	188 (73)	154 (80)	34 (52)
Histology (%)			
PDNEC	63 (24)	37 (19)	26 (39)
Small cell carcinoma	122 (47)	99 (52)	23 (35)
MEEC	21 (8)	16 (8)	5 (8)
Clinically diagnosed NEC	52 (20)	40 (21)	12 (18)
Stage (%)			
IV or recurrent	219 (85)	161 (84)	58 (88)
I–III	39 (15)	31 (16)	8 (12)
Primary site (%)			
Esophagus	85 (33)	85 (44)	
Stomach	70 (27)	70 (36)	
Small bowel	6 (2)	6 (3)	
Colorectum	31 (12)	31 (16)	
Hepato-biliary system	31 (12)		31 (47)
Pancreas	35 (14)		35 (53)
Location of metastases (%)			
Liver	136 (53)	95 (49)	41 (62)
Lymph nodes	131 (51)	103 (54)	28 (42)
Lung	27 (10)	25 (13)	2 (3)
Bone	12 (5)	9 (5)	3 (5)
Brain	1 (0.4)	1 (0.5)	0 (0)
Others	30 (11.6)	26 (14)	4 (6)
Prior surgery (+) (%)	76 (29)	66 (34)	10 (15)

GI, gastrointestinal tract; HBP, hepato-biliary-pancretic system; MEEC, mixed endocrine-exocrine carcinoma; NEC, neuroendocrine carcinoma; PDNEC, poorly differentiated neuroendocrine carcinoma.

Treatment. The most common regimen for first-line chemotherapy was IP (*n* = 160, 62%), followed by EP (*n* = 46, 18%) and fluoropyrimidine-based regimens (*n* = 37, 14%), such as 5-fluorouracil/leucovorin/oxaliplatin combination regimen (FOLFOX) and S-1 (Table 2).

Table 2. First-line chemotherapy regimens

	Eso	Stm	SB	CR	HB	P	Total (%)
Number	85	70	6	31	31	35	258 (100)
Irinotecan+Cisplatin (IP)	71	54	2	15	7	11	160 (62)
Irinotecan+Carboplatin	0	0	0	0	1	0	1 (0.4)
Etoposide+Cisplatin (EP)	4	4	2	2	16	18	46 (18)
Etoposide+Carboplatin	2	0	1	1	0	0	4 (2)
Gemcitabine-based†	0	0	0	0	5	5	10 (4)
Fluoropyrimidine-based†	6	11	1	13	3	3	37 (14)
Others	2	1	0	0	0	0	3 (1)

†Overlapped. CR, colorectum; Eso, esophagus; HB, hepato-biliary system; P, pancreas; SB, small bowel; Stm, stomach.

Survival. The median OS of all 258 patients was 11.5 months. In terms of primary site, the median overall was 13.4 months the esophagus, 13.3 months for the stomach, 29.7 months for the small bowel, 7.6 months for the colorectum, 7.9 months for the hepato-biliary system and 8.5 months for the pancreas (Fig. 2). Subgroups were determined by histological analysis and the median OS in months was calculated: PDNEC (12.6, $n = 63$), SCC (13.0, $n = 122$), MEEC (12.3, $n = 21$) and clinically-diagnosed NEC (9.9, $n = 52$) (Fig. 3). No statistically significant difference in OS was found between the four histology subgroups, including clinically-diagnosed NEC ($P = 0.120$).

Comparison of irinotecan plus cisplatin and etoposide plus cisplatin regimen efficacy. Among the 258 patients, 206 patients (80%) received either IP or EP as their first-line chemotherapy. Table 3 shows the response rate, median PFS and median OS for these 206 patients. In total, 160 patients who received IP showed a better response rate (50 *vs* 28%, $P < 0.001$), longer PFS (median, 5.2 *vs* 4.0 months, $P = 0.033$) and longer OS (median, 13.0 *vs* 7.3 months, $P < 0.001$) than 46 patients who received EP. According to primary site, 142 patients (89%) in the GI subgroup received IP while 34 patients (65%) received EP in the HBP subgroup. The response rate of IP was significantly better than that for EP in the HBP subgroup (39 *vs* 12%, $P = 0.034$), but there were no statistically significant differences with respect to response rate, PFS, or OS between IP and EP in the GI subgroup.

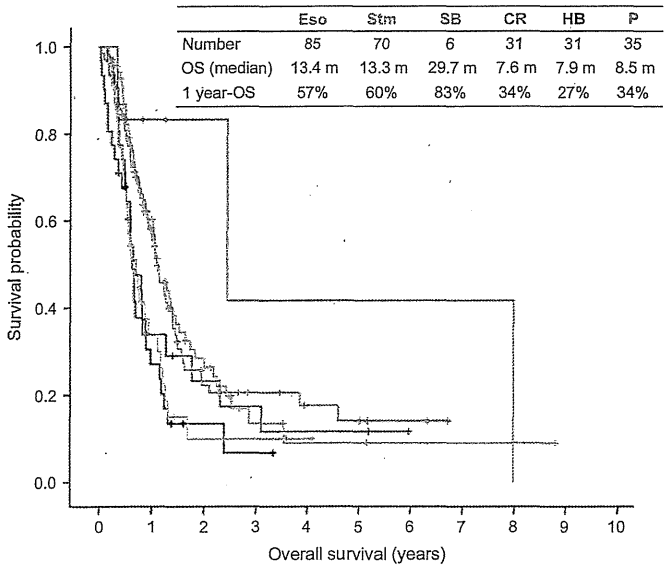

Fig. 2. Kaplan–Meier curves for overall survival according to the primary site. CR, colorectum; Eso, esophagus; HB, hepato-biliary system; OS, overall survival; P, pancreas; SB, small bowel; Stm, stomach.

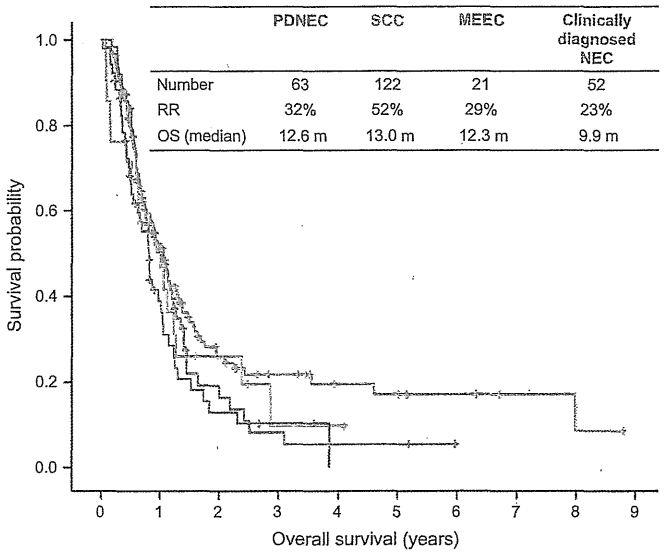

Fig. 3. Kaplan–Meier curves for overall survival according to histology. MEEC, mixed endocrine-exocrine carcinoma; NEC, neuroendocrine carcinoma; OS, overall survival; PDNEC, poorly differentiated neuroendocrine carcinoma; RR, response rate; SCC, small cell carcinoma.

Second-line chemotherapy. Following the failure of IP or EP, 116 patients received second-line chemotherapy. The efficacies of second-line chemotherapy according to the regimen and primary site, GI versus HBP, are shown in Table 4. The efficacy of second-line chemotherapy was slightly better in GI than in HBP patients.

Prognostic factors. In multivariate analysis of prognostic factors for the 206 patients who received EP or IP as their first-line chemotherapy, 23 patients were excluded from the analysis because of no available data on baseline serum LDH

Table 3. Efficacy comparison IP versus EP

	IP	EP	*P*-value
Total			
Number	160	46	
RR	50% (80/160)	28% (13/46)	<0.001†
PFS (median)	5.2 m	4.0 m	0.033‡
OS (median)	13.0 m	7.3 m	<0.001‡
GI			
Number	142	12	
RR	51% (73/142)	75% (9/12)	0.140†
PFS (median)	5.4 m	4.9 m	0.585‡
OS (median)	13.4 m	14.0 m	0.976‡
HBP			
Number	18	34	
RR	39% (7/18)	12% (4/34)	0.034†
PFS (median)	4.4 m	3.7 m	0.056‡
OS (median)	10.1 m	6.9 m	0.050‡

†$\chi 2$. ‡Log-rank test. EP, etoposide plus cisplatin; GI, gastrointestinal tract; HBP, hepato-biliary-pancreatic system; IP, irinotecan plus cisplatin; OS, overall survival; PFS, progression-free survival; RR, response rate.

Table 4. Efficacy of second-line chemotherapy

	Number	RR (%)	PFS† (median)	OS‡ (median)
Regimen				
Amrubicin	25	4	1.9 m	8.3 m
EP or CE	23	17	1.9 m	5.0 m
Irinotecan	21	5	2.2 m	5.9 m
S-1	11	27	2.4 m	12.2 m
IP	5	40	4.8 m	8.7 m
Primary site				
GI	87	15	2.3 m	8.1 m
HBP	29	0	1.6 m	5.1 m
Total	116	11	2.1 m	6.3 m

†PFS from second-line chemotherapy. ‡OS from second-line chemotherapy. CE, etoposide plus carboplatin; EP, etoposide plus cisplatin; GI, gastrointestinal tract; HBP, hepato-biliary-pancreatic system; IP, irinotecan plus cisplatin; OS, overall survival; PFS, progression-free survival; RR, response rate.

levels. The primary site (GI *vs* HBP; HR 0.58, 95% CI 0.35–0.97; $P = 0.039$) and baseline serum LDH levels (not elevated *vs* elevated; HR 0.65, 95% CI 0.46–0.94) were independent prognostic factors for OS (Table 5). There was a tendency towards longer survival in patients treated with the IP regimen, although the difference was not statistically significant (IP *vs* EP; HR 0.80, 95% CI 0.48–1.33; $P = 0.389$).

Discussion

In 2013, the NORDIC group reported a large cohort of GI-NEC patients (NORDIC NEC study) and this study is now regarded as an important reference in the NEC field.[16] The current study is also a large-scale study, conducted subsequent to the NORDIC NEC study. Therefore, it is appropriate to compare the major findings of these two recent studies. Both studies indicated that the primary site and baseline serum LDH levels were important prognostic factors. However, survival of pancreatic NEC patients was extremely poor, with a median OS of 8.6 months in our study, compared with the median OS of 15 months in the NORDIC NEC study. This discrepancy could be due to a difference in patient characteristics and/or tumor biology. In our study, 61% of the pancreatic NEC patients had a Ki-67 index ≥55% compared to only 30% for such patients in the NORDIC NEC study. It should be noted, however, that Ki-67 index data were unavailable for almost half (17/35) of the pancreatic NEC patients in our study (data not shown).

Table 5. Univariate and multivariate analysis for overall survival†

	Univariate analysis		Multivariate analysis	
	P-value	HR (95% CI)	*P*-value	HR (95% CI)
Age				
>60 years old (*vs* <60 years old)	0.069	0.73 (0.52–1.03)	0.541	0.89 (0.62–1.28)
Sex				
Female (*vs* male)	0.143	0.76 (0.52–1.10)	0.766	0.94 (0.61–1.43)
Performance status				
0, 1 (*vs* 2≦)	0.022	0.49 (0.26–0.90)	0.130	0.55 (0.26–1.20)
Lactate dehydrogenase				
Not elevated (*vs* elevated)	0.002	0.58 (0.41–0.82)	0.021	0.65 (0.46–0.94)
Primary site				
GI (*vs* HBP)	<0.001	0.48 (0.33–0.70)	0.039	0.58 (0.35–0.97)
Liver metastasis				
(–) (*vs* (+))	0.033	0.69 (0.49–0.97)	0.119	0.76 (0.53–1.08)
First-line chemotherapy				
IP (*vs* EP)	0.001	0.48 (0.33–0.70)	0.389	0.8 (0.48–1.33)
Prior surgery				
(+) (*vs* (–))	0.141	0.71 (0.45–1.12)	0.636	0.89 (0.55–1.45)

†Number = 183 (In analyzing prognostic factors, 23 patients were excluded for whom baseline serum lactate dehydrogenase level data were not available.) CI, confidence interval; EP, etoposide plus cisplatin; GI, gastrointestinal tract; HBP, hepato-biliary-pancreatic system; HR, hazard ratio; IP, irinotecan plus cisplatin.

First-line chemotherapy regimens were different between the two studies. In our study, IP was the most commonly selected regimen, especially for the GI subgroup, while EP was the most commonly selected regimen in the NORDIC NEC study. This discrepancy might be caused by the different recognition of standard regimens of SCLC between Japan and other countries. In terms of treatment for extensive-stage SCLC, IP demonstrated superiority to EP in a randomized controlled trial conducted in Japan (JCOG9511).[17] IP is still considered a standard therapy for extensive-stage SCLC in Japan, although two subsequent randomized controlled trials conducted outside Japan were not able to confirm these earlier results.[18,19] Therefore, it is essential to determine which chemotherapy regimen, IP or EP, is more effective for NEC of the digestive system. However, the number of published reports on chemotherapy for advanced NEC is limited, and most articles investigate a small number of patients, especially for those treated with IP.[11–15] The definition of NEC has also changed recently. Thus, it is difficult to arrive at a current consensus of standard treatment for advanced NEC based on previous reports.

Our study is the largest study to compare the efficacy of EP and IP. The efficacy of IP was slightly better than EP for the treatment of NEC, even after adjusting patient background by multivariate analysis. Although it can be expected that IP might bring more favorable outcomes than EP, especially in the HBP subgroup, there was a considerable confounding bias between chemotherapy regimens and primary sites. Indeed, most patients in the GI subgroup received IP whereas most patients in the HBP subgroup received EP primarily because of different treatment policies among the institutions. Consequently, it remains difficult to determine which regimen was more effective and whether the optimal chemotherapy regimen depends on the primary site for treating advanced NEC based on the results of our retrospective analysis. According to the consensus report of the National Cancer Institute Neuroendocrine Tumor Clinical Trials planning meeting, GI-NET and pancreatic NET should be examined separately in clinical trials.[20] Although, NET and NEC are different disease entities and there is still no consensus with regard to NEC, prognosis was poorer in pancreatic NEC compared with GI-NEC in the current study. Further study is required to determine the appropriateness of treating all digestive NEC with the same chemotherapy regimen, and whether pancreatic NEC should be investigated separately.

Our analysis indicated only a limited efficacy of second-line chemotherapy. Oral topotecan monotherapy has been recommended for patients with platinum refractory or

relapsed SCLC.[8,21–23] Recently, amrubicin was considered a promising regimen in this setting for SCLC, because it significantly improved the response rate compared with topotecan (31 *vs* 17%).[24] Based on these more recent results, amrubicin was the most commonly-used regimen for second-line chemotherapy in our study. However, its response rate and median PFS were only 4% and 1.9 months, respectively. Amrubicin does not appear to be a promising treatment for platinum-refractory NEC. It is also necessary to establish effective treatment in the second-line setting for NEC of the digestive system.

The present study had several limitations. First, there was wide variation in the quality of pathological diagnosis. In the 2010 WHO classification, the importance of the Ki-67 index is emphasized in the grading of NEN. However, Ki-67 index information was not obtained for 73% of the patients in the present study because many of the subjects in this study had been treated before the recent WHO criteria were published in 2010. Recently, histological differentiation has been recognized as important for diagnosis of NEC and it is well known that poor differentiation is related to poor prognosis. Moreover, the present study included clinically-diagnosed NEC patients. In practice, there are some unavoidable cases where tumor grades are estimated according to histological differentiation and tumor growth velocity because adequate specimens are unavailable for histological grading, particularly specimens obtained by endoscopic ultrasound-guided fine-needle aspiration. In the present study, the prognoses of clinically-diagnosed NEC patients were as poor as for patients in the other histology subgroups. This finding may be one rationale for treating clinically-diagnosed NEC patients in accordance with the treatment of histologically-diagnosed NEC patients. Second, we did not collect toxicity data. These limitations can only be resolved by a well-designed prospective clinical trial. We are currently planning a randomized phase III trial comparing IP with EP for the treatment of advanced NEC of the digestive system.

In conclusion, IP and EP are the most commonly selected treatment regimens in Japan for NEC of the digestive system. The primary site and baseline serum LDH levels are independent prognostic factors for NEC, and IP showed a slightly better tendency for efficacy compared to EP. A prospective randomized controlled trial is required to establish the most appropriate chemotherapy regimen for advanced NEC of the digestive system.

Acknowledgments

The authors extend their sincere appreciation to Dr H. Ishii (Cancer Institute Hospital of Japanese Foundation for Cancer Research), Dr T. Yoshino, Dr M. Ikeda, Dr K. Nakachi (National Cancer Center Hospital East), Dr T. Funakoshi (Shizuoka Cancer Center), Dr T Denda, Dr K. Nakamura (Chiba Cancer Center), Dr H. Nishisaki (Hyogo Cancer Center), Dr C. Katada, Dr M. Kida (Kitasato University Hospital), Dr T. Okuno, Dr A. Ikeda, Dr S. Asari (Kobe University Graduate School of Medicine), Dr I. Hyodo, Dr T. Moriwaki (Institute of Clinical Medicine, Tsukuba University Hospital), Dr H. Kawai, Dr S. Hijioka, Dr T. Hasegawa (Aichi Cancer Center), Dr S. Ohkawa, Dr S. Kobayashi (Kanagawa Cancer Center), Dr A. Hosokawa (Toyama University Hospital), Dr S. Tokunaga (Osaka City General Hospital), Dr Y. Kojima, Dr E. Yokota (National Center for Global Health and Medicine), Dr T. Tsuda (St. Marianna University School of Medicine), Dr M. Matsuda, Dr Y Horita (Toyama Prefectural General Hospital), Dr S. Nakazuru (Osaka National Hospital), Dr K. Nakajima (Miyazaki University Hospital), Dr Y. Komatsu, Dr H. Hayashi (Hokkaido University Hospital), Dr K Matsumoto (Faculty of Medicine, Tottori University), Dr T. Ito, Dr Y. Shiina (Kyushu University Hospital), Ms. K. Kondo, Ms. R. Mukouyama and Ms. H. Hosoi (National Cancer Center Hospital).

Disclosure Statement

Junji Furuse serves as a consultant to Bayer, Chugai Pharma, Eisai, Taiho Pharmaceutical, Ono, Zeria, Boehringer Ingelheim and Kyowa Hakko Kirin and received honoraria from Bayer, Lilly, Taiho Pharmaceutical, Chugai Pharma, Novartis and Yakult; Narikazu Boku received a research grant from Taiho Pharmaceutical, Chugai Pharma, Yakult, Ono, Takeda, Bristol-Myers Squibb and Merck Serono and received honoraria from Yakult, Shionogi, Merck Serono, Ono, Taiho Pharmaceutical, Takeda, Chugai Pharma and Diichi-Sankyo; Takuji Okusaka received honoraria from Lilly, Taiho Pharmaceutical, Novartis, Chugai Pharma, Bayer, Pfizer and Sumitomo and received a research grant from Taiho Pharmaceutical, Lilly, Chugai Pharma, Boehringer Ingelheim, Takeda Bio, Yakult, Kyowa Hakko Kirin, Ono, Otsuka, Eisai, Shizuoka Sangyo, Merck Serono, Astra Zeneca and OncoTherapy Science. The study was funded by the National Cancer Center Research and Development Fund (23-A-22); The corresponding author had full access to all of the data in the study and all authors had final responsibility for the decision to submit for publication.

References

1 Barakat MT, Meeran K, Bloom SR. Neuroendocrine tumours. *Endocr Relat Cancer* 2004; **11**: 1–18.
2 Bosman TF, Carneiro F, Hruban R *et al. WHO Classification of Tumours of the Digestive System*, 4th ed. Lyon: IARC Press, 2010.
3 Terashima T, Morizane C, Hiraoka N *et al.* Comparison of chemotherapeutic treatment outcomes between advanced extrapulmonary neuroendocrine carcinomas and advanced small-cell lung carcinoma. *Neuroendocrinology* 2012; **96**: 324–32.
4 Brennan SM, Gregory DL, Stillie A, Herschtal A, Mac Manus M, Ball DL. Should extrapulmonary small cell cancer be managed like small cell lung cancer? *Cancer* 2010; **116**: 888–95.
5 Wong YN, Jack RH, Mak V, Henrik M, Davies EA. The epidemiology and survival of extrapulmonary small cell carcinoma in South East England, 1970–2004. *BMC Cancer* 2009; **9**: 209.
6 Haider K, Shahid RK, Finch D *et al.* Extrapulmonary small cell cancer: a Canadian province's experience. *Cancer* 2006; **107**: 2262–9.
7 Lee SS, Lee JL, Ryu MH *et al.* Extrapulmonary small cell carcinoma: single center experience with 61 patients. *Acta Oncol* 2007; **46**: 846–51.
8 National Comprehensive Cancer Network National. Comprehensive Cancer Network (NCCN) guidelines. Available from URL: www.nccn.org (Ver. 1 2013).
9 Pavel M, Baudin E, Couvelard A *et al.* ENETS Consensus Guidelines for the management of patients with liver and other distant metastases from neuroendocrine neoplasms of foregut, midgut, hindgut, and unknown primary. *Neuroendocrinology* 2012; **95**: 157–76.
10 Strosberg JR, Coppola D, Klimstra DS *et al.* The NANETS consensus guidelines for the diagnosis and management of poorly differentiated (high-grade) extrapulmonary neuroendocrine carcinomas. *Pancreas* 2010; **39**: 799–800.
11 Moertel CG, Kvols LK, O'Connell MJ, Rubin J. Treatment of neuroendocrine carcinomas with combined etoposide and cisplatin. Evidence of major therapeutic activity in the anaplastic variants of these neoplasms. *Cancer* 1991; **68**: 227–32.
12 Mitry E, Baudin E, Ducreux M *et al.* Treatment of poorly differentiated neuroendocrine tumours with etoposide and cisplatin. *Br J Cancer* 1999; **81**: 1351–5.
13 Iwasa S, Morizane C, Okusaka T *et al.* Cisplatin and etoposide as first-line chemotherapy for poorly differentiated neuroendocrine carcinoma of the hepatobiliary tract and pancreas. *Jpn J Clin Oncol* 2010; **40**: 313–8.
14 Chin K, Baba S, Hosaka H *et al.* Irinotecan plus cisplatin for therapy of small-cell carcinoma of the esophagus: report of 12 cases from single institution experience. *Jpn J Clin Oncol* 2008; **38**: 426–31.
15 Okita NT, Kato K, Takahari D *et al.* Neuroendocrine tumors of the stomach: chemotherapy with cisplatin plus irinotecan is effective for gastric

poorly-differentiated neuroendocrine carcinoma. *Gastric Cancer* 2011; **14**: 161–5.
16 Sorbye H, Welin S, Langer SW *et al.* Predictive and prognostic factors for treatment and survival in 305 patients with advanced gastrointestinal neuroendocrine carcinoma (WHO G3): the NORDIC NEC study. *Ann Oncol* 2013; **24**: 152–60.
17 Noda K, Nishiwaki Y, Kawahara M *et al.* Irinotecan plus cisplatin compared with etoposide plus cisplatin for extensive small-cell lung cancer. *N Engl J Med* 2002; **346**: 85–91.
18 Hanna N, Bunn PA Jr, Langer C *et al.* Randomized phase III trial comparing irinotecan/cisplatin with etoposide/cisplatin in patients with previously untreated extensive-stage disease small-cell lung cancer. *J Clin Oncol* 2006; **24**: 2038–43.
19 Lara PN Jr, Natale R, Crowley J *et al.* Phase III trial of irinotecan/cisplatin compared with etoposide/cisplatin in extensive-stage small-cell lung cancer: clinical and pharmacogenomic results from SWOG S0124. *J Clin Oncol* 2009; **27**: 2530–5.
20 Kulke MH, Siu LL, Tepper JE *et al.* Future directions in the treatment of neuroendocrine tumors: consensus report of the National Cancer Institute Neuroendocrine Tumor clinical trials planning meeting. *J Clin Oncol* 2011; **29**: 934–43.
21 O'Brien ME, Ciuleanu TE, Tsekov H *et al.* Phase III trial comparing supportive care alone with supportive care with oral topotecan in patients with relapsed small-cell lung cancer. *J Clin Oncol* 2006; **24**: 5441–7.
22 von Pawel J, Schiller JH, Shepherd FA *et al.* Topotecan versus cyclophosphamide, doxorubicin, and vincristine for the treatment of recurrent small-cell lung cancer. *J Clin Oncol* 1999; **17**: 658–67.
23 Sørensen M, Pijls-Johannesma M, Felip E, Group EGW. Small-cell lung cancer: ESMO Clinical Practice Guidelines for diagnosis, treatment and follow-up. *Ann Oncol* 2010; **21**(Suppl 5): v120–5.
24 Jotte R, Von Pawel J, Spigel DR *et al.* Randomized phase III trial of amrubicin versus topotecan (Topo) as second-line treatment for small cell lung cancer SCLC (abstract #7000). *J Clin Oncol* 2011; **29**: 453s.

PHLDA3 is a novel tumor suppressor of pancreatic neuroendocrine tumors

Rieko Ohki[a,1], Kozue Saito[a,b], Yu Chen[a,b], Tatsuya Kawase[c], Nobuyoshi Hiraoka[d], Raira Saigawa[a,b], Maiko Minegishi[a,b], Yukie Aita[a], Goichi Yanai[e], Hiroko Shimizu[f], Shinichi Yachida[a], Naoaki Sakata[g], Ryuichiro Doi[h], Tomoo Kosuge[i], Kazuaki Shimada[i], Benjamin Tycko[j], Toshihiko Tsukada[k], Yae Kanai[d], Shoichiro Sumi[e], Hideo Namiki[b], Yoichi Taya[c,l], Tatsuhiro Shibata[f,2], and Hitoshi Nakagama[a,2]

Divisions of [a]Refractory Cancer Research, [c]Radiobiology, [d]Molecular Pathology, [f]Cancer Genomics, and [k]Familial Cancer Research, National Cancer Center Research Institute, Tsukiji 5-1-1, Chuo-ku, Tokyo 104-0045, Japan; [b]Graduate School of Advanced Science and Engineering, Waseda University, 3-4-1 Okubo, Shinjuku-ku, Tokyo 169-8555, Japan; [e]Department of Organ Reconstruction, Institute for Frontier Medical Sciences, Kyoto University, 53 Kawahara-cho, Shogoin, Sakyo-ku, Kyoto 606-8507, Japan; [g]Division of Hepato-Biliary-Pancreatic Surgery, Department of Surgery, Tohoku University Graduate School of Medicine, 2-1, Seiryo-machi, Aoba-ku, Sendai 980-8575, Miyagi, Japan; [h]Department of Surgery and Surgical Basic Science, Graduate School of Medicine, Kyoto University, Yoshida-Konoe-cho, Sakyo-ku, Kyoto 606-8501, Japan; [i]Hepatobiliary and Pancreatic Surgery Division, National Cancer Center Hospital, Tsukiji 5-1-1, Chuo-ku, Tokyo 104-0045, Japan; [j]Institute for Cancer Genetics, Columbia University, New York, NY 10032; and [l]Cancer Research Center of Excellence, Center for Life Sciences, National University of Singapore, Singapore 117456

Edited by Douglas Hanahan, Swiss Federal Institute of Technology Lausanne, Lausanne, Switzerland, and approved May 1, 2014 (received for review October 25, 2013)

The molecular mechanisms underlying the development of pancreatic neuroendocrine tumors (PanNETs) have not been well defined. We report here that the genomic region of the *PHLDA3* gene undergoes loss of heterozygosity (LOH) at a remarkably high frequency in human PanNETs, and this genetic change is correlated with disease progression and poor prognosis. We also show that the *PHLDA3* locus undergoes methylation in addition to LOH, suggesting that a two-hit inactivation of the *PHLDA3* gene is required for PanNET development. We demonstrate that PHLDA3 represses Akt activity and Akt-regulated biological processes in pancreatic endocrine tissues, and that *PHLDA3*-deficient mice develop islet hyperplasia. In addition, we show that the tumor-suppressing pathway mediated by MEN1, a well-known tumor suppressor of PanNETs, is dependent on the pathway mediated by PHLDA3, and inactivation of PHLDA3 and MEN1 cooperatively contribute to PanNET development. Collectively, these results indicate the existence of a novel PHLDA3-mediated pathway of tumor suppression that is important in the development of PanNETs.

p53 | PH domain | everolimus | p53 target gene | mTOR

Neuroendocrine tumors (NETs) arise from cells of the endocrine and nervous systems, and are found in tissues such as lung, pancreas and pituitary (1–3). NETs often produce, store and release biogenic amines and polypeptide hormones, and secretary granules containing these products provide a diagnostic marker for NETs. The mechanisms underlying the development of NETs remain unclear to date, due to the low incidence of these tumors and due to the lack of suitable experimental model systems, including genetically engineered mouse models. Pancreatic NET (PanNET), which is probably the best-studied NET, is the second-most common pancreatic tumor, having an incidence of ~1 per 100,000 individuals. Patients having late-stage PanNET often harbor tumors that are unresectable or metastatic and face limited treatment options. Accordingly, the prognosis of patients having metastatic PanNET is the worst among the NET subtypes, with a 5-y survival rate of 27–43% (1). Recently, the drug Everolimus has shown promise in the treatment of PanNETs (4), providing a significant improvement in progression-free survival. Everolimus is an inhibitor of mammalian target of rapamycin (mTOR), a downstream mediator of the phosphoinositide 3-kinase (PI3K)/protein kinase B (AKT) pathway. The striking efficacy of Everolimus demonstrates the importance of the PI3K/Akt pathway in the pathology of PanNETs.

In agreement with these clinical results, studies on pancreatic endocrine cell lines have identified the PI3K/Akt signaling pathway as a major proliferation and survival pathway in these cells (5). Activated Akt phosphorylates substrates such as mTOR and controls various biological processes, including protein synthesis, proliferation, cell growth, and survival. Regulation of pancreatic islet β-cell proliferation, cell size, and apoptosis by Akt has been demonstrated using various mouse models. For example, transgenic mice overexpressing constitutively active Akt in β-cells exhibit increased β-cell proliferation and cell size and decreased induction of apoptosis (6).

Recently, the results of whole exomic sequencing of 10 PanNET specimens were published, revealing several key genetic alterations (7). In particular, genes in the PI3K/Akt pathway, i.e., TSC2, PTEN, and PIK3CA, were mutated in 15% of PanNETs. However, this represents only a subset of PanNETs, and may not fully explain the remarkable clinical results achieved by Everolimus in the majority of PanNET patients.

Previously, we have shown that Pleckstrin homology-like domain family A, member 3 (PHLDA3) is a novel p53-regulated repressor of Akt. The PHLDA3 contains a PH domain that, we showed, competes with the PH domain of Akt for binding to membrane lipids, thereby inhibiting Akt translocation to the cellular membrane and its activation. We also showed that

Significance

Pancreatic neuroendocrine tumors (PanNETs) are a rare pathology, and molecular mechanisms underlying their development have not been well defined. This article shows that a two-hit inactivation of the *PHLDA3* gene is required for PanNET development: methylation of the locus and loss of heterozygosity. PHLDA3 functions as a suppressor of PanNETs via repression of Akt activity and downstream Akt-regulated biological processes. In addition, the tumor-suppressing pathway mediated by MEN1, a well known suppressor of PanNETs, is dependent on the pathway mediated by PHLDA3, and inactivation of PHLDA3 and MEN1 cooperatively contribute to PanNET development. A novel PHLDA3-mediated pathway of tumor suppression that is important in the development of PanNETs is demonstrated, and the findings may contribute to personalized medicine of PanNET patients.

Author contributions: R.O. designed research; R.O., K. Saito, Y.C., R.S., M.M., Y.A., and H.S. performed research; T. Kawase, N.H., G.Y., S.Y., N.S., R.D., T. Kosuge, K. Shimada, B.T., T.T., Y.K., and S.S. contributed new reagents/analytic tools; R.O. and K. Saito analyzed data; R.O., H. Namiki, Y.T., T.S. and H. Nakagama supervised the research; and R.O. wrote the paper.

The authors declare no conflict of interest.

This article is a PNAS Direct Submission.

[1]To whom correspondence should be addressed. E-mail: rohki@ncc.go.jp.

[2]T.S. and H. Nakagama contributed equally to this work.

This article contains supporting information online at www.pnas.org/lookup/suppl/doi:10.1073/pnas.1319962111/-/DCSupplemental.

PHLDA3 may have a tumor suppressive function (8). However, there has hitherto been no reported role for PHLDA3 in human tumors, and its in vivo function has remained elusive. In this report, we demonstrate that the *PHLDA3* gene is a novel tumor suppressor, inactivation of which can lead to the development of PanNETs. We show that the *PHLDA3* genomic locus undergoes LOH and that the *PHLDA3* promoter is methylated at a high frequency in PanNETs. Furthermore, analysis of *PHLDA3*-deficient mice showed that these mice frequently develop islet hyperplasia as a result of enhanced islet cell proliferation and an increase in islet cell size. Collectively, these results indicate that PHLDA3 functions as a tumor suppressor in PanNETs.

Results

Frequent LOH at the *PHLDA3* Gene Locus in PanNETs. The *PHLDA3* gene is located at 1q31, a locus that has been reported to have a high frequency of LOH in two NETs derived from pancreas: insulinomas and gastrinomas (9, 10). We therefore speculated that the *PHLDA3* locus may undergo LOH in PanNETs, and analyzed the *PHLDA3* locus for LOH using microsatellite markers surrounding the gene in 54 PanNET samples (Fig. 1 *A–D*; clinical diagnosis for each sample is shown in *SI Appendix*, Fig. S1*A*). As shown in Fig. 1*B*, out of 54 PanNETs, 50 samples were informative and 36 samples showed LOH at the *PHLDA3* locus. The incidence of LOH at the *PHLDA3* locus (72%) is remarkably high, and was comparable to the reported LOH incidence of the *Multiple endocrine neoplasia type 1 (MEN1)* gene, which has the highest reported incidence of genomic changes in PanNETs (11). Within the region analyzed, the LOH frequency peaks near the *PHLDA3* locus, suggesting that LOH of the *PHLDA3* gene is critical for PanNET development (Fig. 1*D*). This tendency becomes clearer when samples that exhibit partial LOH within this region (PanNET 1–18) were analyzed (Fig. 1*D*, blue line). A strikingly high incidence of LOH at the *PHLDA3* locus indicates the importance of this PHLDA3-regulated tumor suppression pathway in PanNETs. Most of the PanNETs analyzed in this study are nonfunctional, and we found no associations between *PHLDA3* LOH and specific PanNET type or insulin/glucagon positivity, to the extent that we examined this (*SI Appendix*, Fig. S1).

PHLDA3 and MEN1 Cooperatively Suppress PanNET. The most outstanding genomic aberration previously reported in PanNETs was the mutation and LOH of the *MEN1* gene, a tumor suppressor gene associated with multiple endocrine neoplasia type 1

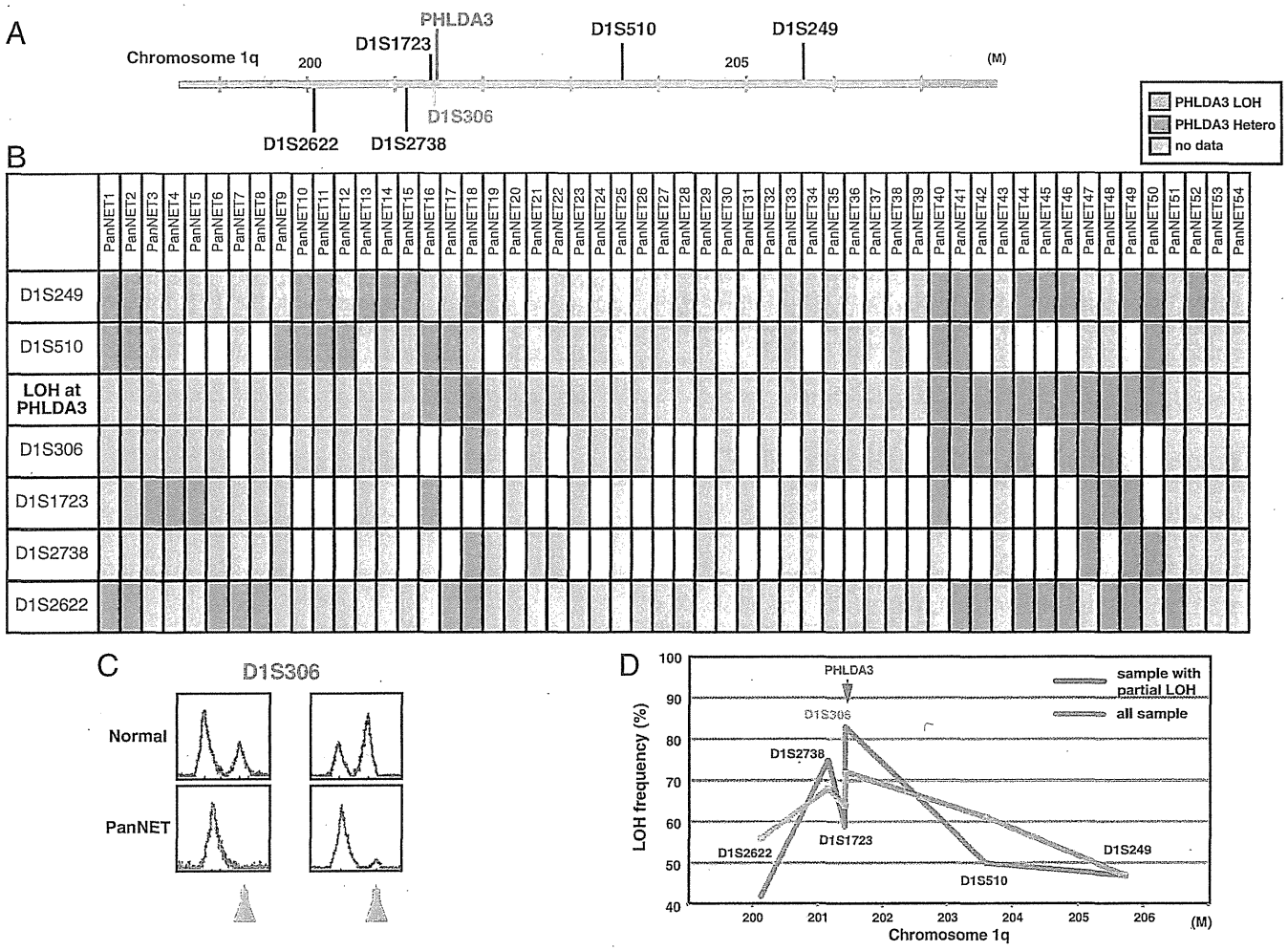

Fig. 1. Frequency of LOH at the *PHLDA3* gene locus in PanNETs. (*A*) Chromosomal locations of *PHLDA3* gene and microsatellite markers used in this study. D1S306 is located just next to the *PHLDA3* gene (32 kb upstream). (*B*) Microsatellite analysis of the *PHLDA3* gene locus region. PanNET samples were analyzed for LOH around the *PHLDA3* gene locus. Because D1S306 is located next to the *PHLDA3* gene, the LOH status of the *PHLDA3* gene was determined from the LOH status of the D1S306 locus. For some loci with no data (not informative or data unavailable), the LOH status of the locus was determined from the surrounding LOH status (shown in faint pink and faint blue). (*C*) Representative microsatellite analysis results. In normal tissues, two peaks derived from maternal and paternal alleles were detected, whereas in tumors, one allele was lost (shown by orange arrows), indicating LOH at the locus. (*D*) LOH frequency for each microsatellite marker. Frequencies from all samples (shown by red line) and frequencies from samples showing LOH partially within the analyzed region (PanNET1-18, shown by blue line) are shown.

(7, 11). It has been reported that ~50% of PanNET cases exhibit LOH of the *MEN1* gene. Therefore, we analyzed whether *MEN1* LOH is observed in our PanNET samples. As shown in Fig. 2 *A* and *B*, 32 samples out of 48 informative samples showed LOH at the *MEN1* locus. Frequent LOH was observed at the *MEN1* locus in our samples (67%), confirming previous studies. We next combined the LOH data for the *PHLDA3* and *MEN1* loci. As shown in Fig. 2*C*, LOH at the *PHLDA3* and *MEN1* loci did not show a mutually exclusive pattern, which would be expected if PHLDA3 and MEN1 were on the same tumor suppressing pathway. Interestingly, we observed a significant frequency of double LOH, i.e., occurring at both the *PHLDA3* and *MEN1* loci (25 of 45 samples, $P < 0.05$ by Fisher's exact test). These data suggest that development of PanNET involves the functional loss of both pathways.

LOH at the *PHLDA3* Locus Is Correlated to Poor Prognosis in PanNET Patients. To select the proper treatment for each PanNET patient, prediction of disease prognosis is important. We observed that LOH at the *PHLDA3* locus was associated with advanced stage PanNETs, whereas absence of LOH was associated with lower tumor grades. These associations were statistically significant ($P < 0.01$, by Fisher's exact test), suggesting that the LOH is associated with a malignant phenotype in PanNETs (Fig. 3*A*). We next analyzed the relationship between LOH at the *PHLDA3* locus and the prognosis of PanNET patients. As shown in Fig. 3*B*, patients exhibiting LOH at the *PHLDA3* locus seemed to have a poorer prognosis compared with the patients without LOH. However, the observed difference did not achieve statistical significance, probably due to the relatively small numbers of patients analyzed. On the other hand, LOH at the *MEN1* locus had no influence on tumor grade or patient survival, as has been reported (7) (Fig. 3 *C* and *D*). It will be necessary to extend these studies with larger numbers of patients before reaching a firm conclusion, however these results suggest that the PHLDA3-regulated pathway, but not the MEN1-regulated pathway, may be a critical determinant of the prognosis of PanNET patients.

The *PHLDA3* Gene Undergoes Aberrant Methylation in Addition to LOH in PanNETs. Because we found frequent LOH at the *PHLDA3* locus in PanNETs, we next examined how the remaining allele is inactivated. The *PHLDA3* gene is mutated in several cancers: 11 mutations in lung, urinary, and large intestine cancer are reported in the COSMIC database (http://cancer.sanger.ac.uk/cancergenome/projects/cosmic), and mutation in lung cancer was reported by Yoo et al. (12). Therefore, we analyzed the *PHLDA3* ORF genomic sequence in our PanNET samples, but did not find any mutations within the coding regions (*SI Appendix*, Fig. S2). We next analyzed *PHLDA3* mRNA expression levels in these PanNETs. As shown in Fig. 4*A*, *PHLDA3* expression was significantly lower in samples showing LOH at the *PHLDA3* locus compared with samples without LOH. We noticed a CpG island overlapping the promoter region and the first exon of the *PHLDA3* gene (Fig. 4*B*). We therefore analyzed whether the methylation status of the *PHLDA3* gene is related to *PHLDA3* transcription levels. Specifically, we analyzed DNA methylation levels within the first exon of the *PHLDA3* gene, because it has been reported that methylation of the first exon is tightly linked to transcriptional silencing (13). Analysis of *PHLDA3* mRNA expression levels in four cancer cell lines revealed that *PHLDA3* is highly expressed in LNCaP and MDA-MB-M468 cells, whereas expression is very low in DLD1 and H1299 cells (Fig. 4*C*). Analysis of DNA methylation levels by methylation-specific PCR revealed detectable methylation only in DLD1 and H1299 cells, cell lines with low *PHLDA3* expression (Fig. 4*D*). It is of note that, in H1299 cells, a human lung NET cell line, *PHLDA3* mRNA expression was remarkably low and methylation was remarkably high. We further treated H1299 cells with 5-aza-C to demethylate the *PHLDA3* gene. As shown in Fig. 4*E*, 5-aza-C treatment resulted in decreased methylation at the *PHLDA3* gene and

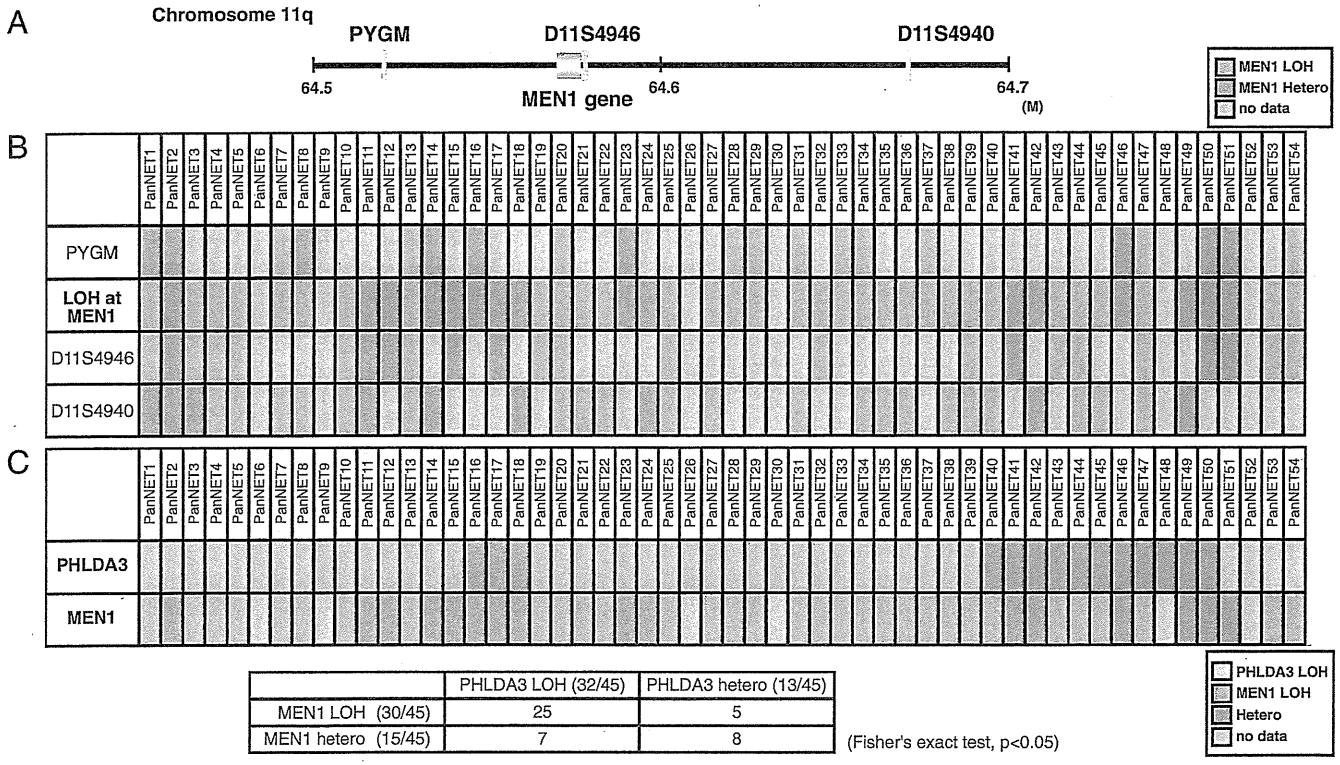

	PHLDA3 LOH (32/45)	PHLDA3 hetero (13/45)
MEN1 LOH (30/45)	25	5
MEN1 hetero (15/45)	7	8

(Fisher's exact test, p<0.05)

Fig. 2. Relationship between PHLDA3 and MEN1 tumor-suppressing pathways. (*A*) Chromosomal locations of the *MEN1* gene and microsatellite markers used in this study. (*B*) Analysis of LOH at the *MEN1* locus. The LOH status of the *MEN1* gene was determined from the LOH status of either of the informative markers. (*C*) Relationship between LOH status of the *PHLDA3* and *MEN1* loci. In total, 45 samples informative for both *PHLDA3* and *MEN1* loci were analyzed.

A

	grade 1or 2	grade 3 or 4
PHLDA3 LOH +	10	21
PHLDA3 LOH-	11	3

(p<0.01, Fisher's exact test)

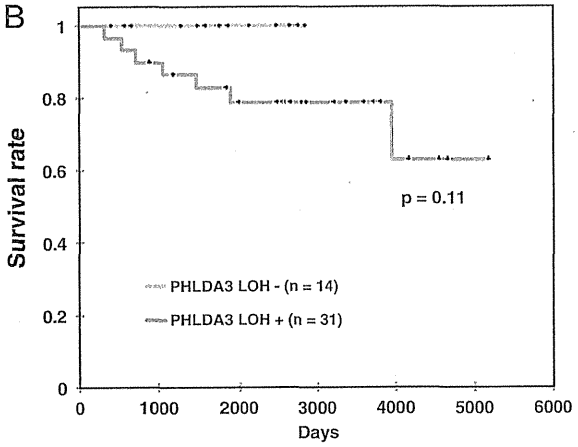

C

	grade 1or 2	grade 3 or 4
MEN1 LOH +	19	19
MEN1 LOH-	4	3

(p=0.73, Fisher's exact test)

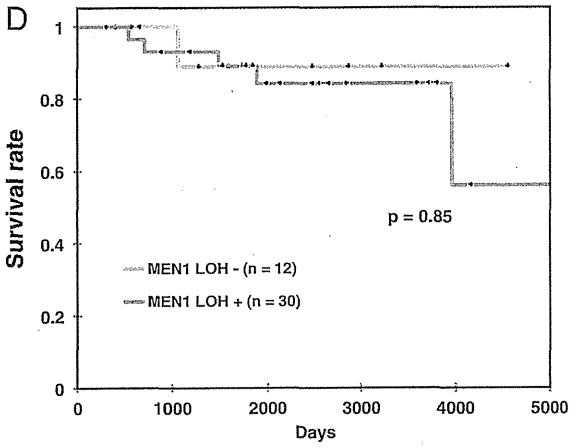

Fig. 3. LOH at the *PHLDA3* and *MEN1* gene locus and progression of PanNETs. (*A*) LOH at the *PHLDA3* gene locus and grade of PanNETs. The *P* value was calculated by Fisher's exact test. (*B*) Kaplan–Meier plots of overall survival of patients with PanNETs. Fourteen or 31 patients without or with *PHLDA3* LOH were analyzed. Wilcoxon test was used to determine the *P* value. (*C*) LOH at the *MEN1* gene locus and grade of PanNETs. (*D*) Kaplan–Meier plot for overall survival of patients with PanNETs. Twelve or 30 patients without or with *MEN1* LOH were analyzed as in *B*.

enhanced expression of *PHLDA3* in a 5-aza-C concentration-dependent manner. A similar result was obtained using a human PanNET cell line A99 (Fig. 4*F*) and the mouse insulinoma cell line MIN6 that has very low PHLDA3 expression (*SI Appendix*, Fig. S3 *A* and *B*). These results indicate that methylation of the *PHLDA3* gene affects *PHLDA3* transcription levels. We then analyzed the methylation status of the *PHLDA3* promoter in PanNET samples that had undergone LOH at the *PHLDA3* locus. As shown in Fig. 4*G*, methylation was not detected in normal pancreas or islets, whereas significant methylation was detected in all LOH+ samples (seven of seven) analyzed. These results show that the *PHLDA3* gene can undergo methylation in addition to LOH in PanNETs, indicating that a two-hit inactivation of the *PHLDA3* gene may often occur. We also analyzed LOH– samples and found detectable levels of methylation in two of four samples (*SI Appendix*, Fig. S4). Thus, the repression of *PHLDA3* expression in LOH– samples due to methylation may also contribute to tumor progression in PanNETs.

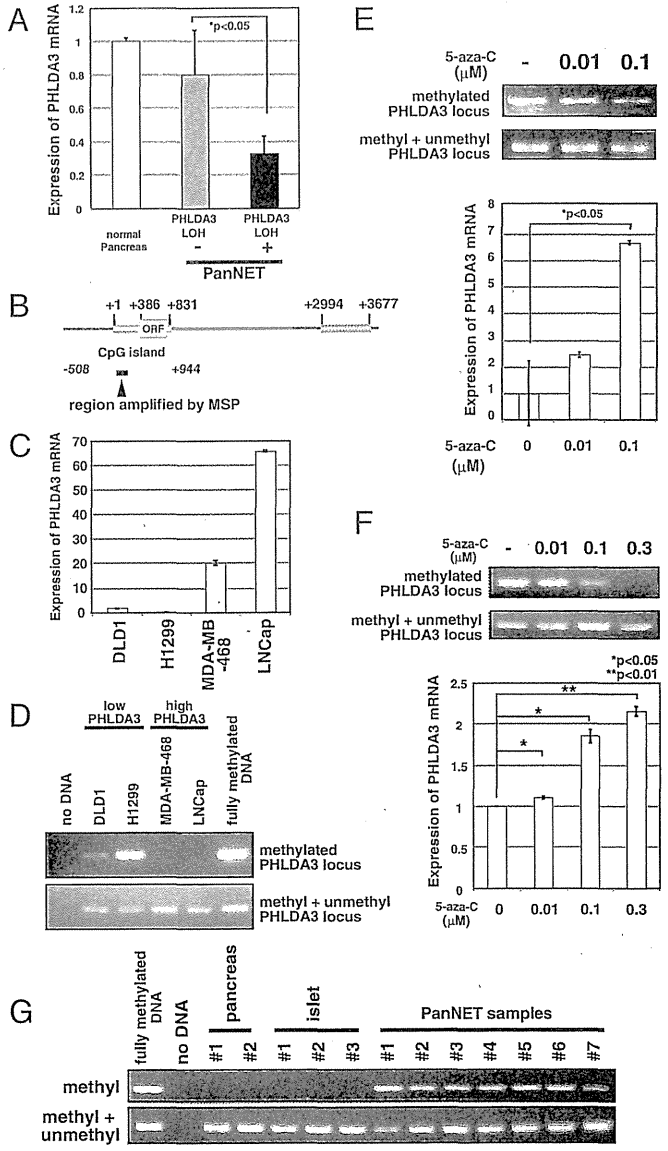

Fig. 4. *PHLDA3* expression and promoter region methylation status in PanNETs. (*A*) *PHLDA3* gene expression in PanNETs. Total RNAs were prepared from normal pancreas and PanNETs. RNA was pooled from 5 normal pancreases for the normal controls. RNA was isolated from PanNET samples with (10 samples) or without LOH (7 samples). Gene expression was quantitated by RT-PCR and normalized to *GAPDH*. (*B*) Genomic organization of *PHLDA3* promoter region and location of CpG island. Wide lines indicate exonic regions of the *PHLDA3* gene (+1 to +831 and +2994 to +3677). (*C*) *PHLDA3* gene expression in cell lines. Gene expression was analyzed as in *A*. (*D*) DNA methylation of the *PHLDA3* promoter. Genomic DNAs from the indicated cell lines were analyzed by methylation-specific PCR. Positions of the primers used in the assay are shown in *B*. Primers designed to amplify methylated DNA (upper panel) or DNA with or without DNA methylation (lower panel) were used. Fully methylated DNA was used as a control. (*E* and *F*) 5-aza-C treatment of Lung NET H1299 cells (*E*) or PanNET A99 cells (*F*). Both genomic DNAs and total RNAs were isolated, and analyzed as in *D* and *A*, respectively. (*G*) Methylation status of *PHLDA3* promoter in normal pancreas, normal isolated islets and PanNETs (samples showing LOH at the *PHLDA3* locus was analyzed). Genomic DNAs were prepared and analyzed as in *D*.

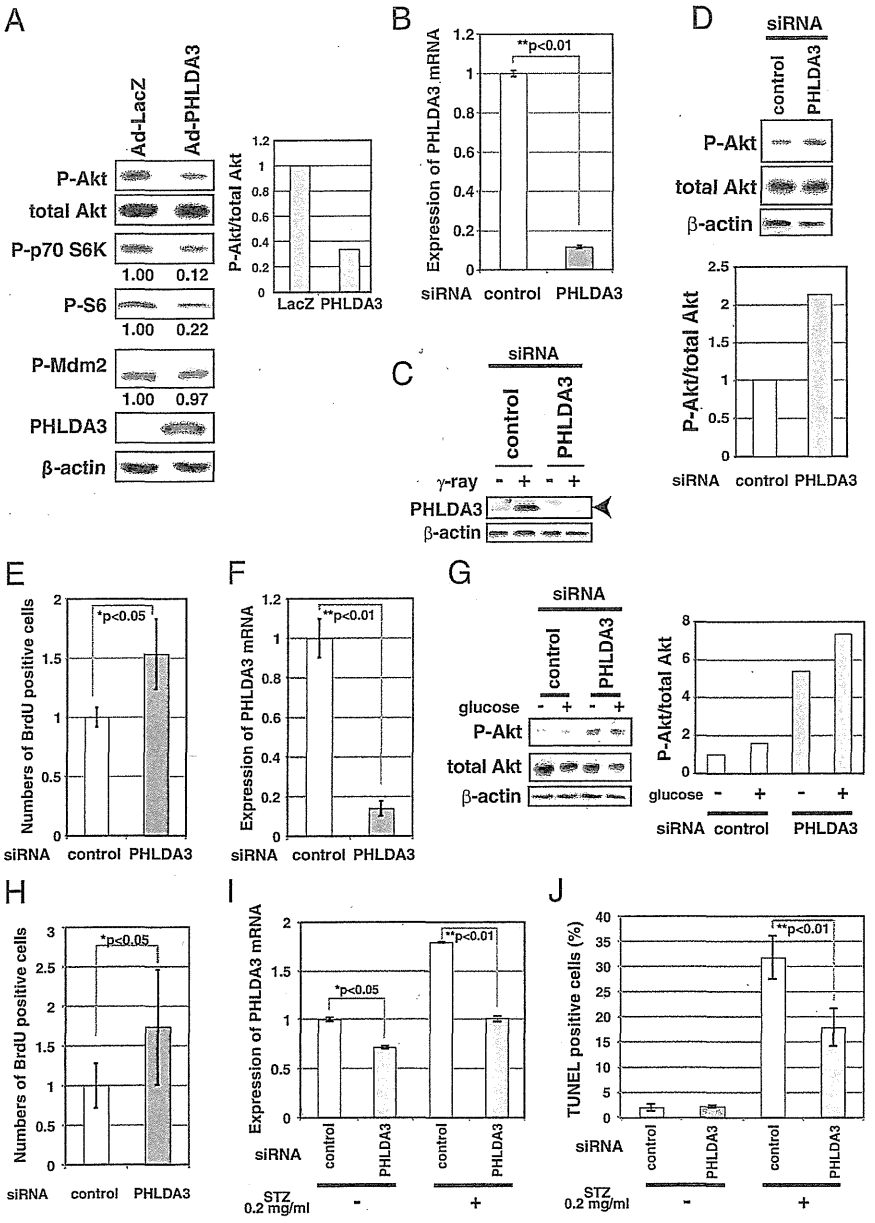

Fig. 5. Effect of PHLDA3 expression on Akt activity, cell proliferation and apoptosis of islet cells. (*A*) Effect of PHLDA3 expression on Akt activity in MIN6 cells. MIN6 cells were transduced with Ad-LacZ or Ad-PHLDA3 at a moi of 35, and harvested 30 h post-infection. Akt activation and phosphorylation of Akt downstream signaling molecules were analyzed by Western blotting and quantified by normalization to total Akt levels (P-Akt) or by β-actin levels (P-p70 S6K, P-S6, P-Mdm2). (*B* and *C*) Efficiency of siRNA inhibition of PHLDA3 expression in RIN cells. RIN cells were transfected with control or PHLDA3 siRNAs. *PHLDA3* mRNA levels were analyzed 31 h posttransfection by quantitative RT-PCR, standardized against β-actin (*B*). PHLDA3 protein levels were also determined 48 h posttransfection by Western blotting (*C*), using cells subjected to γ-ray irradiation (20 Gy) versus untreated. The γ-ray irradiated samples were included to help identify the band representing PHLDA3 protein (PHLDA3 is induced by p53 activation). (*D*) Effect of PHLDA3 expression on Akt activation in RIN cells. RIN cells were transfected as in *B* and Akt activation was analyzed by Western blotting 31 h posttransfection (left) and quantified by normalization to total Akt levels (right). (*E*) Effect of PHLDA3 expression on RIN cell proliferation. RIN cells were transfected as in *B*, and labeled with BrdU for 3 h and harvested 28 h post transfection. BrdU positive cells were quantified by using Ziva Ultrasensitive BrdU assay. (*F*) siRNA suppression of *PHLDA3* expression in primary islet cells. Isolated primary islet cells were transfected with control or PHLDA3 siRNA, harvested 30 h post transfection, and *PHLDA3* mRNA levels were analyzed by quantitative RT-PCR as in *B*. (*G*) Effect of PHLDA3 expression on Akt activation in primary islet cells. Cells were transfected with siRNA as in *F* and 48 h post-transfection were treated with glucose (30 mM) for 20 min. Levels of Akt activation were analyzed as in *D*. (*H*) Effect of PHLDA3 expression on primary islet cell proliferation. Cells were transfected as in *F*, labeled with BrdU for 4 h and harvested 30 h post transfection. BrdU positive cells were analyzed as in *E*. (*I* and *J*) Effect of PHLDA3 expression on STZ-induced apoptosis of primary rat islets. Isolated islets were pooled from three rats, and transfected with control or PHLDA3 siRNA. At 75 h posttransfection, islets were treated with STZ (20 μg/mL) for 30 min. Islets were then cultured overnight, and total RNAs were prepared and *PHLDA3* expression was analyzed by quantitative RT-PCR as in B (*I*), or subjected to TUNEL staining and analyzed by FACS (*J*).

PHLDA3 Controls Akt Activity, Cell Proliferation, and Apoptosis of Islet Cells. PanNETs are derived from pancreatic islet endocrine cells. It is well known that, in islet β cells, Akt signaling plays a central role in promoting cell growth and inhibiting apoptosis (5). Therefore, in β cells, loss of PHLDA3 function may result in the hyperactivation of Akt oncogenic signaling, and thus lead to tumor progression. To analyze the function of PHLDA3 in islet β cells, we examined RIN and MIN6 cells, cell lines derived from pancreatic β cells (Fig. 5 *A–E*). Whereas RIN cells have detectable levels of PHLDA3 expression, MIN6 has very low PHLDA3 expression (*SI Appendix*, Fig. S3*A*). We first used a gain-of-function approach to confirm that PHLDA3 functions as a repressor of Akt in MIN6 cells. As shown in Fig. 5*A*, expression of PHLDA3 resulted in decreased Akt activation levels and decreased phosphorylation of signaling molecules downstream of Akt. Similar results were obtained using *PHLDA3*$^{-/-}$ mouse embryonic fibroblasts (MEFs, *SI Appendix*, Fig. S5). Next, we knocked down PHLDA3 expression in RIN cells using siRNA against PHLDA3 (Fig. 5 *B* and *C*), and observed increased Akt activation and cell proliferation (Fig. 5 *D* and *E*). We observed similar results in normal primary rat islet cells, i.e., knockdown of PHLDA3 expression resulted in activation of Akt (with or without glucose stimulation) and significant enhancement of cell proliferation (Fig. 5 *F–H* and *SI Appendix*, Fig. S6). Next, we analyzed the effect of PHLDA3 expression on the apoptosis of islet cells induced by Streptozotocin (STZ), a chemical that is particularly toxic to insulin-producing β cells (14). We observed that although inhibition of *PHLDA3* expression by siRNA was relatively poor in isolated rat islets (Fig. 5*I*), this knockdown significantly reduced the number of apoptotic cells caused by STZ treatment (Fig. 5*J*). Collectively, these results demonstrate that PHLDA3 controls Akt activity, cell growth, and the apoptosis of islet cells.

Development of Hyperplastic Islets in *PHLDA3*-Deficient Mice. To analyze the effect of PHLDA3 deficiency on islets in vivo, we examined the pancreases of *PHLDA3*-deficient mice. Differences in islet sizes were not detected in 3-mo-old *PHLDA3*$^{+/+}$ or *PHLDA3*$^{-/-}$ mice (*SI Appendix*, Fig. S7). However, in 6-mo-old *PHLDA3*$^{-/-}$ mice, we found significantly fewer islets that were smaller than 0.01 mm^2 and significantly more islets that were larger than 0.01 mm^2, compared with *PHLDA3*$^{+/+}$ mice (Fig. 6 *A* and *C*).

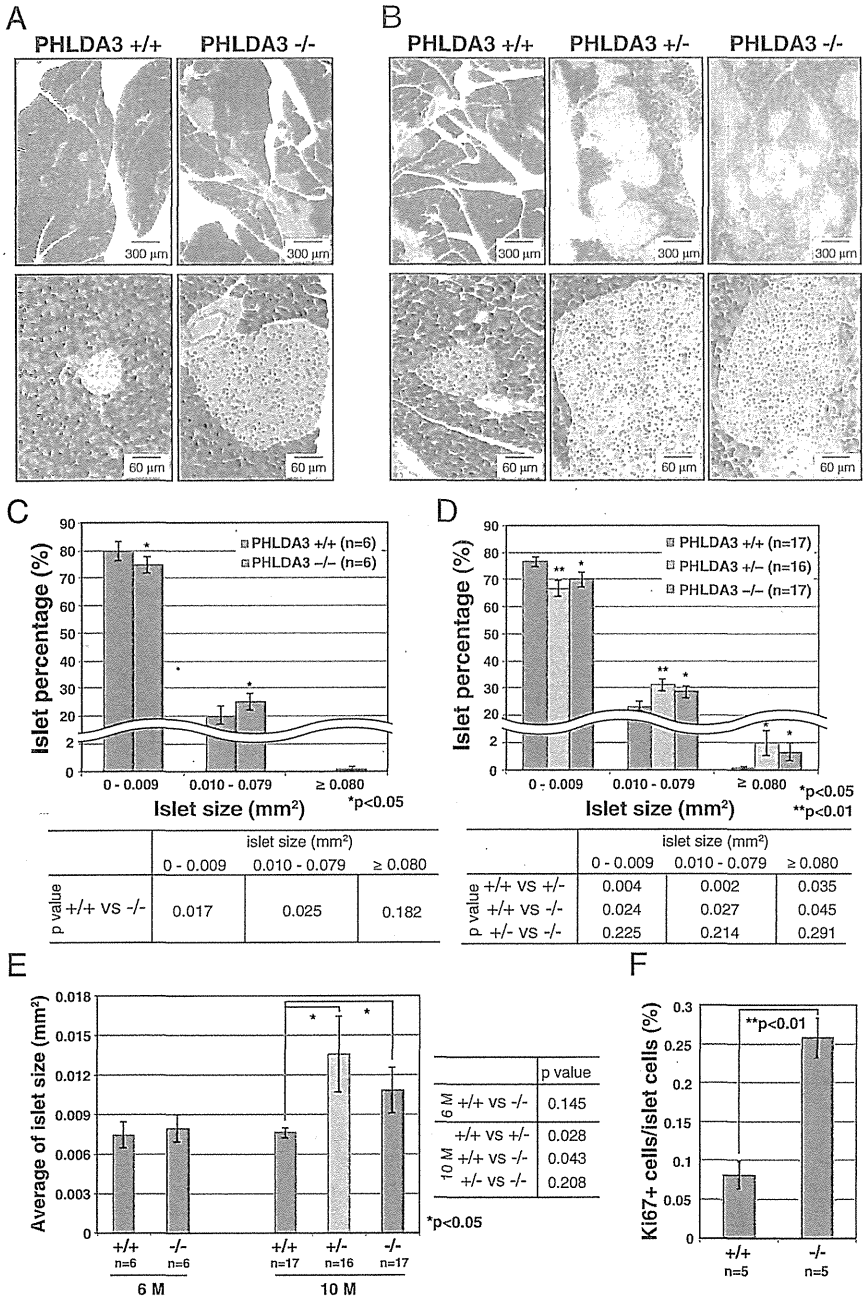

Fig. 6. Hyperplastic islets in *PHLDA3*-deficient mice. Six-month-old (21- to 31-wk-old) (*A*, *C*, and *E*) and 10-mo-old (39- to 49-wk-old) (*B* and *D*–*F*) mice were analyzed. (*A* and *B*) Hematoxylin and eosin staining of islets from wild-type, heterozygote and *PHLDA3*-deficient mice (*A*, 6-mo; *B*, 10-mo). (*C*–*E*) Calculation of islet sizes. Islet areas were calculated from hematoxylin and eosin-stained pancreas sections. One (6-mo-old mice) or three pancreas sections (10-mo-old mice; sections separated by more than 20 μm *z* axis) were analyzed per mouse. Islet areas from indicated numbers (n) of mice were analyzed. Size distributions of islets (*C*, 6-mo; *D*, 10-mo) and average islet sizes (*E*; 6- and 10-mo-old) are shown. The *P* values between $PHLDA3^{+/+}$ and $PHLDA3^{+/-}$ or $PHLDA3^{-/-}$ were calculated and are shown (*$P < 0.05$; **$P < 0.01$). (*F*) Quantitation of Ki67-positive cells. Pancreas sections from indicated numbers (n) of mice were analyzed. Islet nuclei number and Ki67-positive nuclei number were counted and the percentage of Ki67-positive cells was calculated. (**$P < 0.01$) Representative images are shown in *SI Appendix*, Fig. S4.

However, the overall average islet size at 6 mo was not significantly different between $PHLDA3^{+/+}$ and $PHLDA3^{-/-}$ mice (Fig. 6*E*). At 10 mo, abnormally large islets (larger than 0.08 mm^2) were frequently found (Fig. 6 *B* and *D*), and the average islet sizes were significantly larger in 10-mo-old $PHLDA3^{+/-}$ and $PHLDA3^{-/-}$ mice compared with $PHLDA3^{+/+}$ mice (Fig. 6*E*). Thus, a difference in islet sizes between $PHLDA3^{+/+}$ and $PHLDA3^{-/-}$ mice appears to emerge between 3 and 10 mo of age. We stained the islets with Ki67 antibody and found significantly more Ki67-positive cells in $PHLDA3^{-/-}$ islets compared with the $PHLDA3^{+/+}$ islets (Fig. 6*F*; representative images are shown in *SI Appendix*, Fig. S8). These data show that loss of PHLDA3 expression results in enhanced proliferation of islet cells.

Enhanced Proliferation of β Cells and Altered Glucose Metabolism in *PHLDA3*-Deficient Mice. The islets were further stained with anti-insulin and anti-glucagon antibodies to determine the numbers of β and α cells, respectively, within the islets. Normal murine islets have β cells in the center of the islet and α cells at the periphery surrounding the β cells (as shown in $PHLDA3^{+/+}$ islets in Fig. 7*A*). However, in the hyperplastic islets of $PHLDA3^{+/-}$ and $PHLDA3^{-/-}$ mice, huge numbers of β cells and relatively small numbers of α cells were often observed, and the hyperplastic islets often showed abnormal islet architecture, with few α cells at the periphery of the islets (Fig. 7*A*). We calculated the areas occupied by α and β cell types to determine which of these had increased. As shown in Fig. 7*B*, the mean percentage area occupied by β cells was significantly higher in $PHLDA3^{-/-}$ islets. The area occupied by β cells was also significantly high in large $PHLDA3^{-/-}$ islets (larger than 0.05 mm^2) compared with that seen in large islets infrequently found in $PHLDA3^{+/+}$ mice (Fig. 7*B*). Because we had found a significantly higher number of proliferating cells in $PHLDA3^{-/-}$ islets (Fig. 6*F*), we stained the islets with anti-Ki67, -insulin, and -glucagon antibodies to identify which cell types within the islets were proliferating. As shown in Fig. 7*C*, we found that most Ki67-

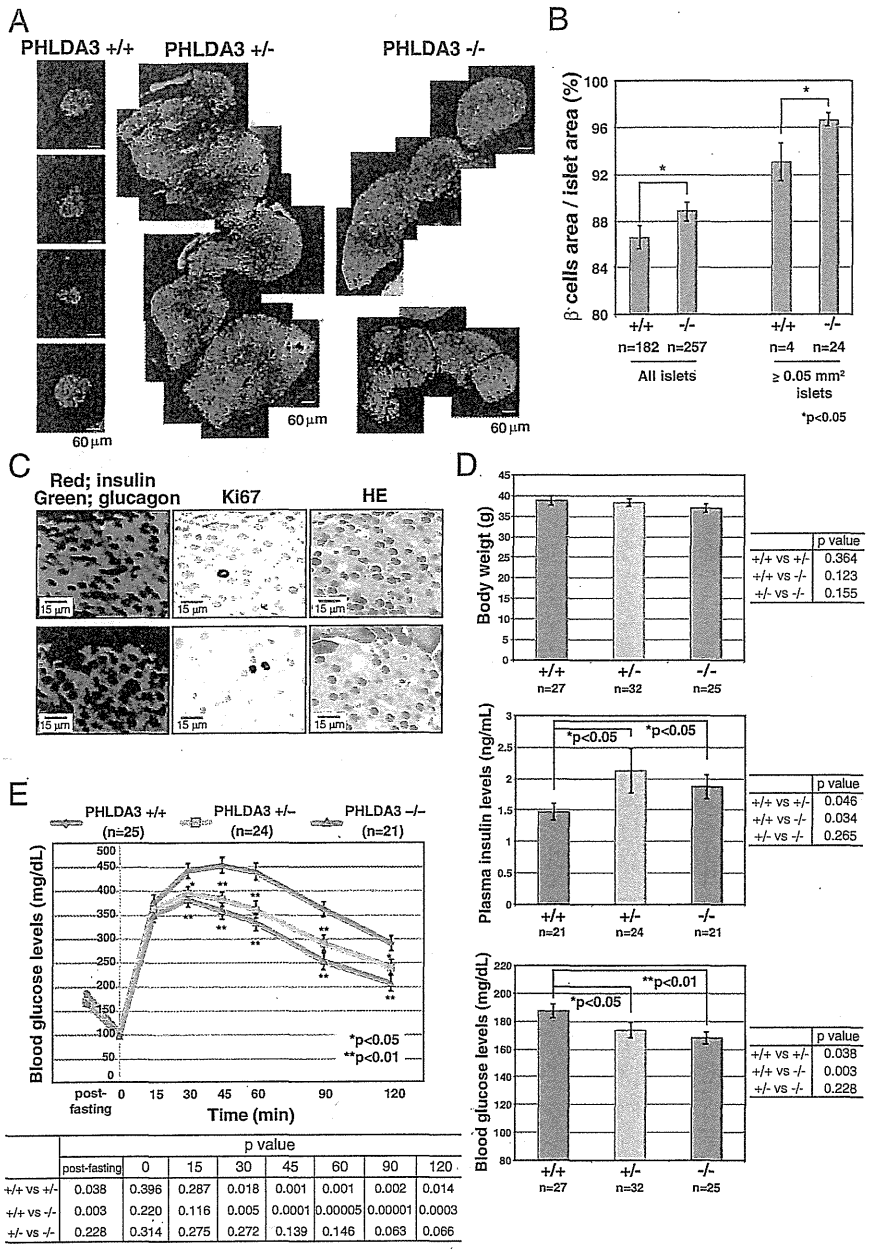

Fig. 7. Proliferation of β cells in the islets of *PHLDA3*-deficient mice. Ten-mo-old (39- to 49-wk-old) mice were analyzed. (*A*) Distribution of β and α cells in pancreas sections. Pancreas sections were stained with antibodies to identify β cells (anti-insulin; red) and α cells (anti-glucagon; green). Representative images of hyperplastic islets from *PHLDA3*$^{+/-}$ and *PHLDA3*$^{-/-}$ mice are shown. (*B*) Percent area occupied by β cells. Pancreas sections were stained as in *A*, and areas occupied by α- and β-cells in indicated numbers of islets from *PHLDA3*$^{+/+}$ (five mice were analyzed) and *PHLDA3*$^{-/-}$ (six mice were analyzed) were calculated and percentages of β-cell areas in the islets were determined. Semihyperplasic islets and hyperplastic islets (larger than 0.05 mm^2 islet area) were separately calculated and shown at the right. (*$P < 0.05$; **$P < 0.01$). (*C*) Proliferation in pancreas sections. Serial pancreas sections of *PHLDA3*$^{-/-}$ mice were stained with anti-insulin and anti-glucagon, anti-Ki67 and HE, to determine the cell types that are Ki67 positive. Representative images are shown. (*D*) Body weight, blood glucose and insulin levels. Indicated numbers (n) of mice were analyzed. Plasma insulin levels and blood glucose levels were determined in blood from tail vein samples, and were determined twice for each mouse. Mice were fed ad libitum. (*$P < 0.05$; **$P < 0.01$). (*E*) Glucose tolerance test (GTT). Indicated numbers (n) of overnight-fasted mice were subjected to GTT by i.p. injection of glucose (2 mg/g body weight). GTT was performed twice for each mouse. The *P* values between *PHLDA3*$^{+/+}$ and *PHLDA3*$^{+/-}$ or *PHLDA3*$^{-/-}$ were calculated and are shown in the panels (*$P < 0.05$; **$P < 0.01$). The differences between *PHLDA3*$^{+/-}$ and *PHLDA3*$^{-/-}$ were not significant ($P > 0.05$).

positive cells were β cells in *PHLDA3*$^{-/-}$ islets. Taken together, these data show that islet β cell proliferation is enhanced in *PHLDA3*-deficient islets.

It would be expected that abnormal proliferation of β cells would result in the excess production of insulin, leading to altered glucose metabolism in *PHLDA3*-deficient mice. As shown in Fig. 7*D*, although the *PHLDA3* genotype had no influence on body weights, 10-mo-old *PHLDA3*$^{+/-}$ and *PHLDA3*$^{-/-}$ mice had higher plasma insulin and lower blood glucose levels compared with age-matched wild-type mice under fed conditions. Similar results were obtained in 6-mo-old fed mice (*SI Appendix*, Fig. S9*A*) and in 10-mo-old fasted mice (*SI Appendix*, Fig. S9*B*). Therefore, we performed glucose tolerance tests and found significant enhancement of glucose tolerance in *PHLDA3*$^{+/-}$ and *PHLDA3*$^{-/-}$ mice (Fig. 7*E*). These data show that loss of PHLDA3 expression results in enhanced proliferation of islet cells, especially β cells, and consequential increase of insulin secretion.

We further characterized *PHLDA3*$^{-/-}$ islets using several β cell markers: the endocrine cell marker chromogranin A (*SI Appendix*, Fig. S10), the β cell differentiation marker Glut2 (*SI Appendix*, Fig. S11), and deposition of IAPP (islet amyloid polypeptide; *SI Appendix*, Fig. S12). None of these markers showed significant difference compared with *PHLDA3*$^{+/+}$ islets, indicating that *PHLDA3*$^{-/-}$ islets retain normal β cell characteristics, to the extent we examined.

***PHLDA3*-Deficient Islets Have Enhanced Akt Activity and Larger Cell Size, and Are Resistant to Apoptosis.** We further analyzed the effects of PHLDA3 deficiency on several Akt-regulated biological processes. We first confirmed reduction or loss of *PHLDA3* expression in *PHLDA3*$^{+/-}$ and *PHLDA3*$^{-/-}$ mice islets (Fig. 8*A*). We found that activation of Akt and phosphorylation of its downstream molecules were augmented in *PHLDA3*$^{-/-}$ islets (Fig. 8*B*). It has been reported that enhanced Akt activity has an effect on islet cell size (5, 6). We therefore analyzed islet cell size in *PHLDA3*$^{+/+}$, *PHLDA3*$^{+/-}$, and *PHLDA3*$^{-/-}$ mice. As shown in Fig. 8*C*, islet cell size was significantly increased in *PHLDA3*$^{-/-}$ and *PHLDA3*$^{+/-}$ mice. We next analyzed the sensitivity of *PHLDA3*$^{-/-}$ islets to apoptosis. Wild-type or *PHLDA3*$^{-/-}$ mice were treated with STZ for 5 consecutive days to produce β cell injury. It is known that STZ-induced apoptosis of β

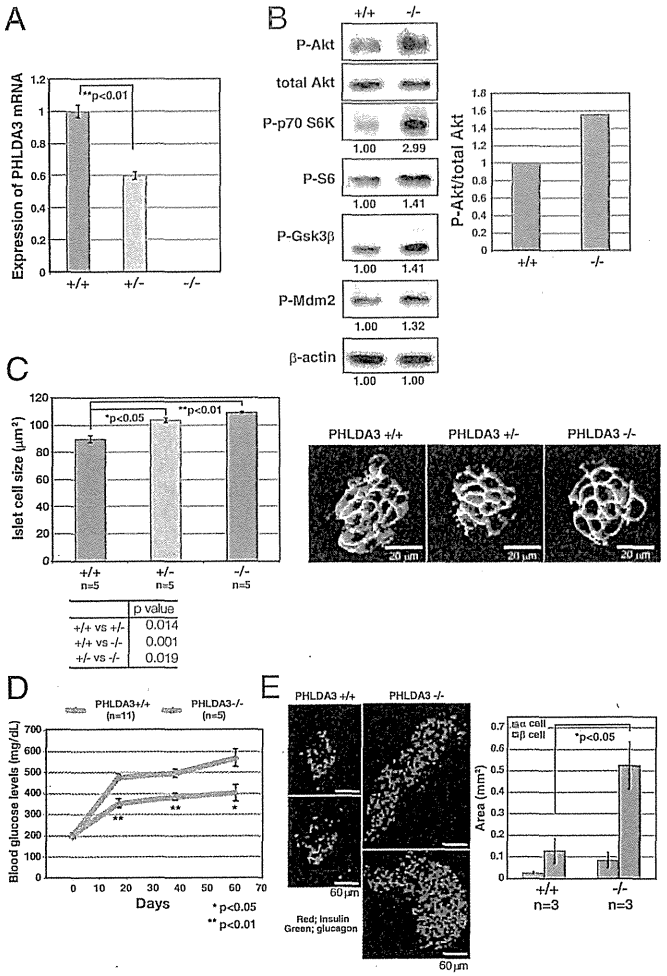

Fig. 8. Akt activation in islets of *PHLDA3*-deficient mice. (*A*) *PHLDA3* mRNA expression in isolated islets. Islets were isolated from $PHLDA3^{+/+}$, $PHLDA3^{+/-}$, and $PHLDA3^{-/-}$ mice, and analyzed for *PHLDA3* expression by quantitative RT-PCR, normalized to β-actin. (*B*) Akt activity and phosphorylation of Akt downstream signaling molecules in isolated islets. Akt activation and phosphorylation of Akt downstream signaling molecules were analyzed by Western blotting and quantified by normalization to total Akt levels (P-Akt, *Right*) or by β-actin levels (P-p70 S6K, P-S6, P-GSK3β, and P-Mdm2). (*C*) Islet cell size in *PHLDA3*-deficient mice. (*Left*) Indirect immunofluorescence staining of Glut2 in pancreas section from 10-mo-old mice. (*Right*) Islet areas and nuclei numbers were calculated, and mean islet cell sizes were determined from one hematoxylin- and eosin-stained pancreas sections per indicated numbers (n) of mice. The *P* values between $PHLDA3^{+/+}$ and $PHLDA3^{+/-}$ or $PHLDA3^{-/-}$ were calculated and shown in the panels ($*P < 0.05$; $**P < 0.01$). The difference between $PHLDA3^{+/-}$ and $PHLDA3^{-/-}$ was also significant ($P < 0.05$). (*D*) Blood glucose levels in streptozotocin-induced diabetic mice. Indicated numbers (n) of $PHLDA3^{+/+}$ or $PHLDA3^{-/-}$ mice were injected i.p. with STZ for 5 consecutive days. Blood glucose levels were determined at different time points as indicated after administration of STZ. ($*P < 0.05$; $**P < 0.01$). (*E*) Distribution of β and α cells in STZ-treated $PHLDA3^{+/+}$ and $PHLDA3^{-/-}$ mice. (*Left*) Sections were stained with antibody against insulin (β cell marker; red) and glucagon (α cell marker; green) and representative images are shown. Pancreas sections of three $PHLDA3^{+/+}$ and three $PHLDA3^{-/-}$ mice were analyzed. (*Right*) For each mouse, α-cell and β-cell areas were calculated from one pancreas section. ($*P < 0.05$.)

cell results in the elevation of blood glucose, and can thereby experimentally induce type I diabetes in mice. We analyzed blood glucose levels at the indicated times following STZ treatment, and STZ administration resulted in the effective elevation of blood glucose levels in wild-type mice, whereas elevation was diminished in $PHLDA3^{-/-}$ mice (Fig. 8*D*). When we calculated β cell and α cell areas in STZ-treated mice, we observed a significant increase in the area occupied by β cells in *PHLDA3*-deficient mice, showing that PHLDA3 is required for the efficient induction of β cell apoptosis by STZ (Fig. 8*E*). These results demonstrate that PHLDA3 controls Akt activity, cell size, and apoptosis of islet cells in vivo.

Discussion

In this report, we have shown that PHLDA3 is a candidate tumor suppressor in PanNETs. We observed that the LOH of the *PHLDA3* gene locus in human PanNETs occurs at a remarkably high frequency and is comparable to that of the *MEN1* gene locus, the gene reported to be most frequently affected in PanNETs (15). We also showed that LOH at the *PHLDA3* gene locus is associated with disease progression and poor prognosis in PanNETs. In contrast, LOH/mutation of *MEN1* was found to be unrelated to the prognosis of PanNET patients, both in this and in a previous study (7). These results show that the PHLDA3-regulated tumor suppression pathway is relevant to the progression and malignant phenotype of PanNETs and the poor prognosis of PanNET patients. Because PHLDA3 is a repressor of Akt, we propose that inhibition of the Akt pathway would improve the prognosis of PanNET patients exhibiting LOH of *PHLDA3*. This possibility is supported by the reported clinical efficacy of the Akt pathway inhibitor Everolimus, which has been shown to improve the survival of PanNET patients significantly. Everolimus treatment was approved in Japan only from 2011, and therefore none of the patients in our study had received Everolimus. We speculate that patients who are positive for *PHLDA3* LOH and have a poor prognosis may benefit most from Everolimus treatment. Furthermore, determination of *PHLDA3* LOH status could serve as a diagnostic measure to select patients who should receive Everolimus. Thus, it will be important to conduct a prospective study to analyze the effect of Everolimus in patients with or without *PHLDA3* LOH.

We have shown that PHLDA3 regulates Akt activity and various Akt-regulated biological processes, i.e., cell proliferation, cell size, and apoptosis, in cultured cell lines and in vivo endocrine cells. Several laboratories have generated transgenic mice that specifically express active Akt in β cells (6, 16). These mice developed hyperplastic islets, but did not develop malignant PanNETs (17). Likewise, we have shown that loss of PHLDA3 and the resulting activation of Akt leads to hyperplastic islet development, but not to the development of PanNETs. Although Akt activation is observed in various cancers and contributes to tumorigenesis and tumor progression, the conclusion derived from these experiments is that activation of Akt pathway alone is insufficient to cause PanNETs unless combined with an oncogenic event in a second pathway. In human PanNETs, double LOH of *PHLDA3* and *MEN1* is frequently observed. In these cells, loss of PHLDA3 function, i.e., activation of Akt, is combined with loss of MEN1 function to promote PanNET tumorigenesis, and loss of PHLDA3 function particularly contributes to the progression of PanNETs. It would therefore be interesting to generate mice that are doubly deficient in *PHLDA3* and *MEN1* to analyze whether the islet phenotypes are more pronounced and the hyperplastic islets more prone to malignancy.

We observed hyperplastic islets in *PHLDA3* heterozygote (+/−) mice as well as *PHLDA3*-deficient (−/−) mice. This observation suggests that *PHLDA3* is haplo-insufficient for the suppression of endocrine cell proliferation. We have previously shown that PHLDA3 expression represses Akt activity in a dose-dependent manner, consistent with the possibility that loss of a single *PHLDA3* allele could lead to enhanced Akt activation and enhanced proliferation of endocrine cells (8). However, we have also shown that in human PanNETs, the *PHLDA3* locus undergoes methylation in addition to LOH, suggesting that two hits on the *PHLDA3* gene is required for human PanNET development. We assume that loss of both *PHLDA3* alleles, and consequent stronger activation of Akt, may be required to exert a tumorigenic phenotype. Future studies should examine the islet phenotypes of $PHLDA3^{+/-}$ and $PHLDA3^{-/-}$ in a $MEN1^{-/-}$ back-

ground. We expect that, in a *MEN1*$^{-/-}$ background, *PHLDA3*$^{-/-}$ mice would develop PanNETs more frequently than in *PHLDA3*$^{+/-}$ mice. In addition, because we found association of LOH at the *PHLDA3* locus in both nonfunctional and functional human PanNETs, whether nonfunctional PanNETs develop in these mice is an interesting issue.

We previously identified *PHLDA3* as a p53 target gene. In the present study, we show that the *PHLDA3* locus undergoes frequent LOH in PanNETs, a tumor type in which p53 mutations are rare (3, 7). Recently it has been reported that among the various target genes of p53, *PHLDA3* displays prominent tumor suppressor activity (18). Therefore, in tumors harboring a p53 mutation, loss of p53-regulated *PHLDA3* expression may significantly contribute to tumor progression, whereas in tumors without a p53 mutation, loss of the *PHLDA3* gene itself may drive oncogenesis. Interestingly, global methylation profiling of prostate cancer specimens has revealed significant methylation of the *PHLDA3* gene in these cancers (19). In addition, in the COSMIC database, 11 PHLDA3 mutations in several cancers are reported. All mutations are located within the PH domain of PHLDA3, and nonsynonymous mutations may result in loss of Akt repressing ability. Therefore, in addition to inactivation by methylation, these and other mutations that result in a functional loss of PHLDA3 may contribute to some cancers.

In summary, our results show that PHLDA3 is a novel tumor suppressor of PanNET, and PHLDA3 and MEN1 cooperatively suppress its development. PHLDA3 represses Akt activity in islet cells and hyperplastic islets are found in both *PHLDA3*$^{+/-}$ and *PHLDA3*$^{-/-}$ mice. Collectively, our data illustrates the importance of the PHLDA3-regulated tumor suppression pathway in PanNETs.

Materials and Methods

Cell Lines, Cell Culture, Transfection, Adenovirus Infection, and Soft Agar Colony Formation Assay. Cell lines used in this study were: LNCaP (human prostate cancer), MDA-MB-M468 (human breast cancer), DLD1 (human colorectal cancer), H1299 (human lung NET), A99 (human PanNET, ref. 20), RIN (rat pancreatic β cell), and MIN6 (mouse pancreatic β cell). Cell culture and transfection was performed as described (21). The siRNAs were introduced using RNAiMAX (Invitrogen). ON-target plus control and ON-target plus PHLDA3-targeting siRNAs were purchased from Dharmacon Research. Adenovirus infection was performed using previously described adenoviruses expressing LacZ or N-terminally HA-tagged PHLDA3 (8). Everolimus (AdooQ BioScience) was added to cultures at the indicated concentrations. For soft agar colony formation assays, cells were seeded in 3-cm dishes with a bottom layer of 0.5% agarose and a top layer of 0.33% agarose, both in complete media. The assay was performed in triplicate for each sample. Colonies were photographed after 9 (H1299) or 10 (MIN6) days of incubation. Colonies were counted in three to five different views from each plate to calculate average values. The total numbers of colonies larger than 100 (MIN6) or 200 (H1299) pixels were counted per view.

Western Blotting Analysis. Cells were lysed in lysis buffer [50 mM Tris·HCl (pH 8.0), 1% Nonidet P-40, 250 mM NaCl, 50 mM NaF, 1 mM Na_3VO_4, 1 mM protease inhibitor (PMSF, aprotinin, leupeptin) and 1 mM DDT]. Whole cell lysates were subjected to protein quantification and analyzed by Western blotting. To detect PHLDA3, 20 μg of whole cell lysates (WCL) were loaded. To detect other proteins, 5 μg of WCL were loaded. Antibodies used in this study were: anti-Akt rabbit polyclonal antibody, anti-phospho-Akt (S473) rabbit monoclonal antibody, anti-p70S6K rabbit monoclonal antibody, anti-phospho-p70S6K (T389) rabbit polyclonal antibody, anti-phospho-S6 (S240/244) rabbit monoclonal antibody, anti-phospho-Gsk3β (S9) rabbit polyclonal antibody, anti-phospho-Mdm2 (S166) rabbit polyclonal antibody from Cell Signaling Technology, anti-actin mouse monoclonal antibody from SIGMA from Santa Cruz Biotechnology, anti-PHLDA3 goat polyclonal antibody from Abcam, anti-HA monoclonal antibody (clone 12CA) from Roche Diagnostics.

Reverse Transcription and Real-Time PCR. Reverse transcription was carried out using kits from Invitrogen following the manufacturer's instructions (SuperScript First-Strand Synthesis System for RT-PCR). Total RNA (0.2–5 μg) was used for reverse transcription. Reverse-transcribed cDNAs were subjected to real-time PCR, which was performed with a LightCycler 480 Instrument (Roche Diagnostics). For the detection of PHLDA3 (human; Hs00385313_m1, mouse; Mm00449846_m1, rat; rat; Rn01483684_m1), beta actin (mouse; Mm00607939_s1, rat; Rn00667869_m1) and GAPDH (human; Hs02758991_g1, mouse; Mm99999915_g1), TaqMan probe from Applied Biosystems was used.

BrdU Incorporation Assay and Measurement of Cell Number. BrdU-positive cells were quantified using the Ziva Ultrasensitive BrdU assay (Jaden BioScience). This assay detects the incorporation of BrdU using a labeled anti-BrdU antibody and detection substrate in an ELISA format. By this assay, a small fraction of proliferating cells within a large population of nonproliferating cells can be detected. Cell numbers were analyzed by using CellTiter-Glo Luminescent Cell Viability Assay (Promega). Using this assay, viable cells are determined by quantitation of ATP, an indicator of metabolically active cells.

Flow Cytometry and TUNEL Assay. Apoptosis of islet cells was quantitated by the TUNEL reaction using the In Situ Cell Death Detection kit, Fluorescein (Roche Diagnostics) followed by flow cytometry. Flow cytometry analysis was performed using a FACS Calibur instrument (Becton Dickinson).

Tumor Samples Used in the Study, and DNA and RNA Extraction from Primary Tumor Samples. The tumor samples used in this study were surgically resected at the National Cancer Center Hospital (44 samples; PanNET1-18, 24–47, 52, 53), Kyoto University Hospital (6 samples; PanNET19-23, 51), or Kagawa University Hospital (4 samples; PanNET 48–50, 54) between 1993 and 2012. Histological grading of the tumors were determined based on the classification of World Health Organization 2004. This study was approved by the Institutional Review Board of the National Cancer Center, Tokyo. Clinical and pathological data were obtained through a detailed retrospective review of the medical records of all patients with PanNET. Five-micrometer sections of paraffin-embedded tissues were subjected to DNA extraction. Total RNA was extracted from frozen normal pancreas and tumor samples using an RNeasy mini kit (Qiagen).

Microsatellite Analysis. Microsatellite analysis was performed basically as described (8). We used six primer pairs labeled with FAM that amplify microsatellite loci to achieve accurate detection of LOH at the *PHLDA3* locus (Fig. 1*A*). For the *MEN1* locus, three primer pairs were used (Fig. 2*A*). Amplified PCR products were analyzed with a 3100 automated sequencer (Applied Biosystems). Collected data were analyzed with GeneScan and Genotyper software (Applied Biosystems), and allele sizes and peak heights were calculated. The genotype was determined to be heterozygous if two bands of different sizes were obtained from normal tissues. A ratio of the two peaks in tumor DNA of less than 0.7 in comparison with the corresponding ratio of the two peaks in nontumor DNA was considered as allelic loss.

5-aza-dC Treatment and Methylation-Specific PCR. Cells were seeded at a density of 3×10^5 cells (H1299 and A99) or 3×10^6 (MIN6) cells per 10-cm dish on day 0 and treated with freshly prepared 5-aza-dC (Sigma-Aldrich) for 24 h on days 1, 3, and 5. After each treatment, cells were placed in fresh medium and harvested on day 6. Genomic DNA was extracted and subjected to bisulfite conversion using EZ DNA Methylation kit (Zymo research). Fully methylated controls were prepared by methylating genomic DNA with SssI methylase (New England Biolabs). Methylation-specific PCR (MSP) was performed basically as described (22). MSP was performed using the specific primer sets shown below. BS-F and R primers were used to amplify DNA with or without methylation. MSP-F and R primers were used to amplify methylated DNA.

BS-F: GTAGATAGAGTTTAGGGGAGTAAGAG

BS- R: CTCTACCCCAACTAACCCAACCC

MSP-F: GAGGGTTGGTTAGGGTAGGAATGTG

MSP-R: ACTCCCCTAAACTCTATCTACACAC

Mice Used in This Study. Generation of *PHLDA3*-deficient mice was reported (23). Briefly, a *PHLDA3*neo targeting vector was obtained by cloning a 6-kb upstream KpnI fragment and a 6-kb downstream HindIII/NotI fragment into pPNT1. The resulting deletion (nucleotides 579–2,096 of GenBank accession no. AF151099) eliminates all of exon 1 and part of exon 2, thus deleting the entire *PHLDA3* coding region. *PHLDA3*$^{-/-}$ mice were generated by crossing the heterozygotes. MEFs were isolated and maintained as described (24). Mouse experiments were performed in a specific pathogen-free environment at the National Cancer Center animal facility according to institutional guidelines, and all of the animal experiments were approved by the Committee for Ethics in Animal Experimentation at the National Cancer Center.

Blood Glucose, Plasma Insulin Measurement, and Glucose Tolerance Tests. Blood glucose levels were determined with blood samples from tail vein